Chapter 4

Advanced feeds for mm-wave antenna systems

Authors: Jorge Teniente, Juan Carlos Iriarte, Iñigo Ederra and Ramon Gonzalo, Public University of Navarra, Spain

4.1 Introduction

Millimetre-wave antenna systems have traditionally required high performance feeds in order to fulfil its stringent requirements. Therefore, this goal has been achieved by corrugated horns. However, in the last years new applications mainly in the communication area have driven the use of other types of antenna feed with slightly reduced performance but simpler manufacturing and reduced cost. The simplicity of manufacturing is especially critical as frequency increases and in fact corrugated horns are extremely difficult and expensive to manufacture at submm-wave frequencies.

This chapter will cover the different alternatives currently used for mm-wave and submm-wave antenna feeds: corrugated horns, smooth walled horns where multi-flare angle horns and splined horns will be introduced as alternatives to corrugated horns at mm-wave and submm-wave frequencies. Finally, the chapter will finish with the perspectives and actual research results regarding metamaterial based feeds towards future applications.

4.2 Advanced corrugated horn antennas

This section describes the actual corrugated feed horn technologies employed at mm-wave frequencies. It begins explaining the principles of the electrical behaviour of the electrical fields inside a corrugated waveguide. The hybrid mode basis as a tool to help in the analysis of corrugated horns and the relation between waveguide modes and free space gaussian modes are explained to understand the behaviour of the different types of corrugated horn antennas.

In fact, corrugated feed horns are difficult to manufacture as frequency increases and usually are not usually used above W band. The reason is that their manufacture results quite difficult being necessary to use for the manufacture expensive electroforming techniques or even stacked rings if the weight is not an important parameter.

4.2.1 Introduction to corrugated horn antennas

Corrugated horns have become now-a-days the preferred choice of feed antennas for use in high restrictive applications. This is because of their superior radiation performance, their high copolar radiation pattern symmetry and their low crosspolarisation. Usually they are the preferred choice when a superior radiation pattern is needed for a specific application and the main market is spaceborne communications and science missions in fact.

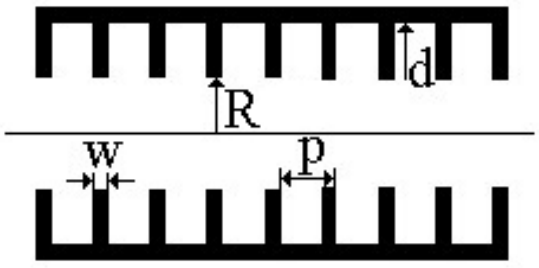

Figure 4.1. Corrugated waveguide

The operation principle of corrugated horns can be physically explained by considering the way in which the corrugated wall affects the field distribution inside a corrugated waveguide (see fig. 4.1). It can be demonstrated that the corrugations change the fields travelling through the waveguide to produce the desirable radiating properties of axial beam symmetry, low sidelobes and low crosspolarization [1].

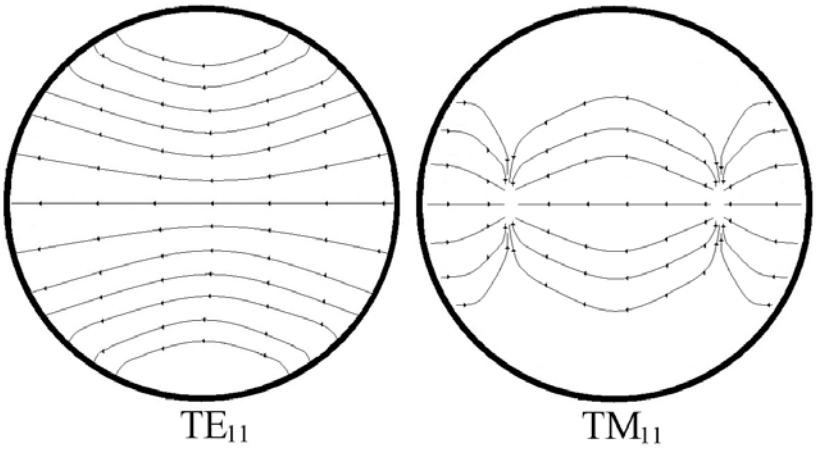

Figure 4.2. TE_{11} and TM_{11} aperture electric fields

A linear electric field for low crosspolar level will be desirable but it cannot be obtained with smooth waveguides that only support pure transverse electric (*TE*) or a pure transverse-magnetic (*TM*) modes. These modes have the aperture electric field lines curved (see fig. 4.2). Therefore, a multimode horn should be designed. In [2], a special horn design to obtain an appropriate mode mixture by the addition of TE_{11} and TM_{11} modes in a particular proportion and phase was presented, but its bandwidth was very narrow.

It is well known that to define properly the field inside a circular waveguide the most known basis used is the *TE* and *TM* mode family which are a direct solution of the wave equation inside a smooth circular waveguide [3]. But if the waveguide is corrugated it could be also useful to define the field inside the waveguide by the family of hybrid modes *HE* and *EH* (those modes which doesn't present pure transverse components along the waveguide). So, in fact we can choose to define the field inside the corrugated horn antennas in terms of *TE* and *TM* modes or in terms of *HE* and *EH* modes.

Theoretically, the hybrid modes HE_{1n} present at the aperture of a circular waveguide perfectly linear electric field lines, (see Fig. 4.3). It is interesting to aid in the knowledge of corrugated horn antennas to deepen in the understanding of hybrid modes of a corrugated waveguide.

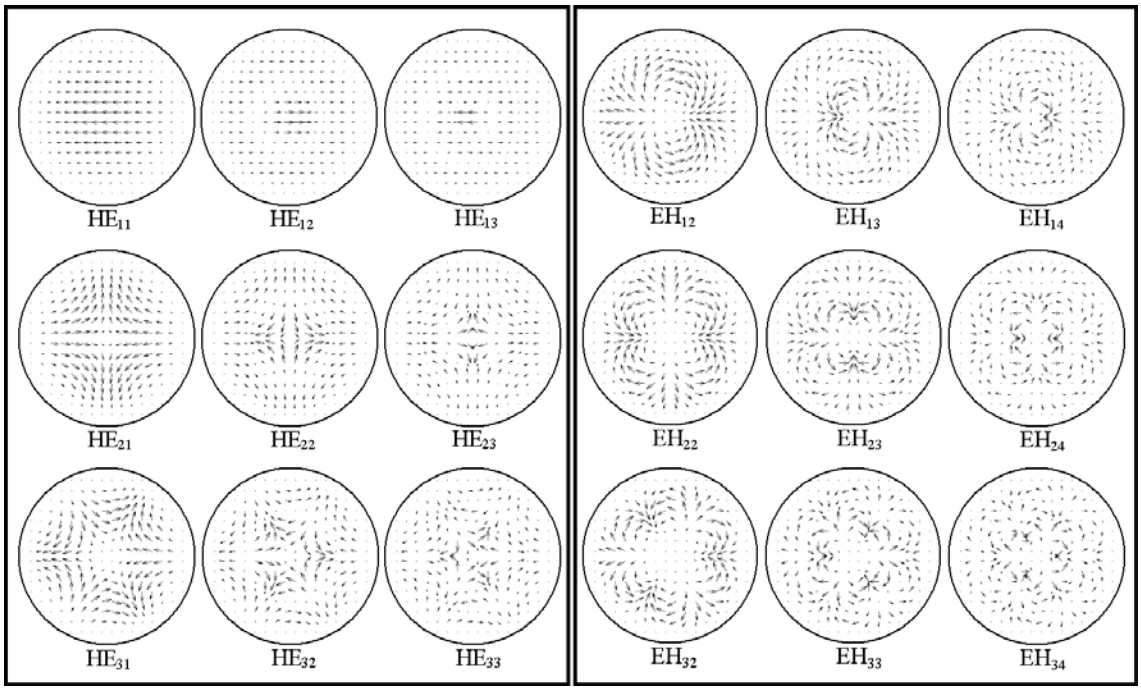

Figure 4.3. HE_{mn} and EH_{mn} aperture electric fields

As a corrugated horn is fed via a circular waveguide that propagates the fundamental mode of a circular waveguide (TE_{11}) and considering that a corrugated horn is composed of symmetrical radius variations of such circular waveguide at its throat, the only hybrid modes to consider in a corrugated waveguide or horn antenna are those with $m=1$, HE_{1n} and EH_{1n}.

Then, the HE_{11} mode is the fundamental mode of a corrugated waveguide and presents linear electric field at the aperture, (see fig. 4.3). The mode can be expressed as a combination of TE and TM modes, as a generating basis that they are. Commonly, in the bibliography [1], the HE_{11} mode is supposed to be a combination of *85 %* of TE_{11} and *15 %* of TM_{11} with the adequate phase shift between them. But in fact, this mode mixture is not perfect, (*99.19 %* efficient with HE_{11} mode), the perfect mode mixture in terms of smooth waveguide modes can be seen in table 4.1.

TE modes	$TE_{11}\begin{cases}84.496\% \\ 0^o\end{cases}$	$TE_{12}\begin{cases}0.082\% \\ 180^o\end{cases}$	$TE_{13}\begin{cases}3.58\cdot10^{-3}\% \\ 180^o\end{cases}$	$TE_{14}\begin{cases}4.94\cdot10^{-4}\% \\ 180^o\end{cases}$
TM modes	$TM_{11}\begin{cases}14.606\% \\ 0^o\end{cases}$	$TM_{12}\begin{cases}0.613\% \\ 0^o\end{cases}$	$TM_{13}\begin{cases}0.121\% \\ 0^o\end{cases}$	$TM_{14}\begin{cases}0.039\% \\ 0^o\end{cases}$

Table 4.1. HE_{11} mode decomposition in terms of TE_{1n} and TM_{1n} modes

It is also important to know the radiation properties of hybrid modes to understand the behaviour of corrugated horn antennas. In fig. 2.8, the radiation diagrams of the first HE_{1n} and EH_{1n} modes is represented. In that figure we can see, for example, the effect on the crosspolar component if a EH_{1n} mode is excited inside a corrugated horn. Or also from the same figure, the excellent radiation properties of the HE_{11} with nearly null crosspolar component and with a radiation diagram with quite low sidelobes can be observed.

The HE_{11} fundamental corrugated waveguide hybrid mode is then an excellent mode for radiation purposes. For a common corrugated horn with oversized aperture, the radiated crosspolarized level will be very low, the aperture illumination efficiency will be high and the sidelobe level will be also quite low, (see fig. 4.4).

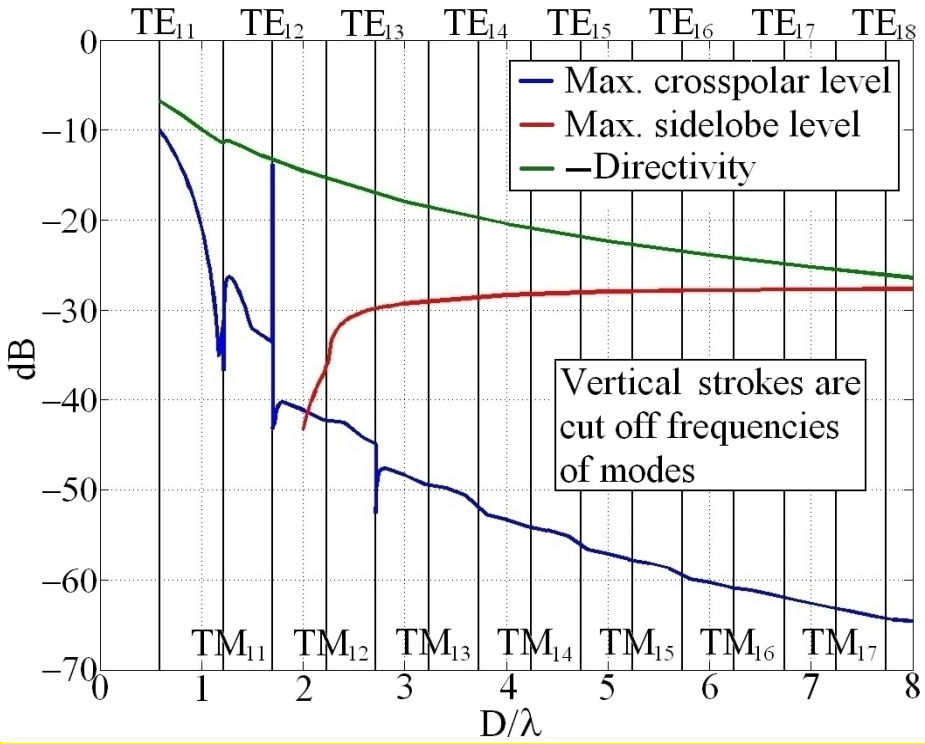

Figure 4.4. Radiation properties of the HE_{11} hybrid mode against aperture diameter (D)

As a conclusion of the radiation properties of the HE_{11} hybrid mode, it can be said that this mode is an excellent mode to be excited at the aperture of a corrugated waveguide, and it offers low crosspolar levels and quite low sidelobe levels. However, if very low sidelobes are required for a high restrictive antenna, and its necessary to maintain low crosspolar levels, we would need several higher order HE_{1n} modes to be present at the aperture of the horn with appropriate amplitude and phase shift between them. This is in fact the purpose of advanced corrugated feed horn designs via optimization of the profiles and the corrugation parameters.

However, it is well known that one of the best ways to define a free space radiation from a horn antenna is by means of the paraxial free space modes, the gaussian modes, which are a solution of the paraxial free space equation. It is important also to remark the radiation similarity between the fundamental gaussian mode of a certain and the HE_{11} mode at a certain diameter aperture. In fact, the fundamental gaussian beam mode can be decomposed in terms of smooth waveguide modes (TE_{mn} and TM_{mn}) and also in terms of corrugated waveguide hybrid modes (HE_{mn} and EH_{mn}) at a certain horn aperture radius (R) with respect to the beamwaist (w_0) of the gaussian beam at such horn aperture.

From figure 4.5 we can see that the fundamental gaussian mode can be expressed completely as a combination of TE_{1n} and TM_{1n} smooth waveguide modes and also as a combination of HE_{1n} hybrid modes. At this point, it should be noted that HE_{11} mode has been always known as a gaussian-like mode because its field is nearly a pure gaussian, in fact it is up to *98.1 %* efficient with a fundamental gaussian beam of $R/w_0=1.554$ ($w_0/R=0.6435$) (see Fig. 4.5b). To obtain at the aperture of a corrugated horn antenna a

high efficient fundamental gaussian beam mode (this implies lower sidelobes), more hybrid modes must be present at the horn aperture as it has been introduced. This aspect will be covered in the following lines regarding advanced corrugated feed horn design.

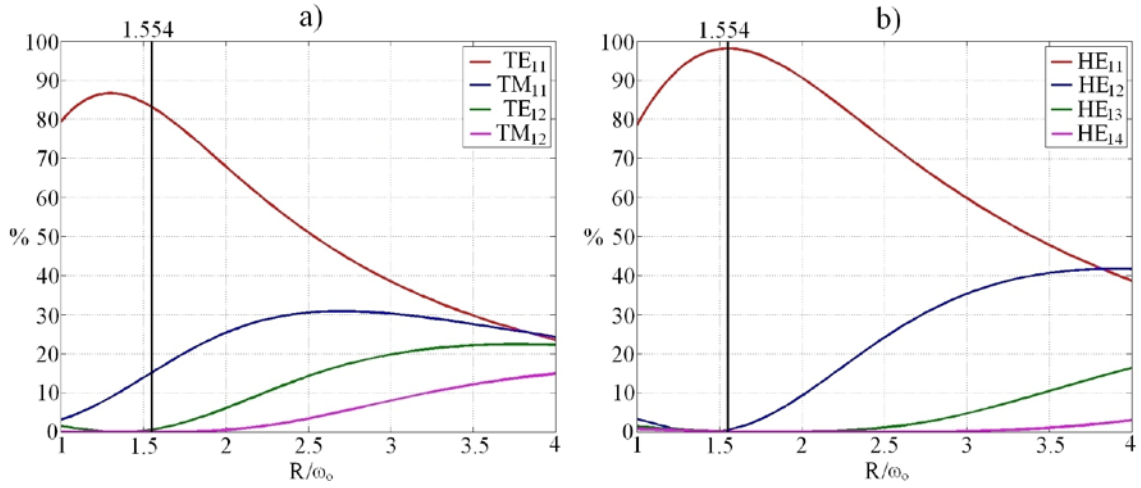

Figure 4.5. a) Fundamental gaussian mode decomposition in terms of TE and TM
b) Fundamental gaussian mode decomposition in terms of HE and EH

4.2.2 Radially corrugated feed horn antennas

The design of circular horn antennas was based, for a long time, in the control of the waveguide mode mixture to excite an HE_{11} hybrid mode. It is well known from the previous part that this hybrid mode can be made up of approximately a combination of *85% TE_{11}* and *15% TM_{11}* smooth circular waveguide modes with an appropriate relative phasing between them. The starting field distribution is usually the TE_{11} mode of the circular waveguide under monomode operation, and by means of a proper step or taper in the horn radius, the right amount of TM_{11} (amplitude and phase) was excited (Potter type horns) [1,4,5]. To get this mixture with nice radiating features, two main parameters had to be considered: the output diameter and the horn length. Since the coupling coefficient between waveguide modes is directly related to the waveguide slope change, for a given output radius that fixes the desired beamwidth, the change in horn length allows the designer to select the appropriate phasing in the *85%* of TE_{11} and *15%* of TM_{11} mode mixture obtaining the appropriate sidelobe and crosspolarization minimum levels. This type of horn antennas has been extensively used in the past and are known as Potter type horns, [4]. Its drawback is the reduced bandwidth a design of this type could cover.

Another technique is based on corrugated circular waveguides and takes profit of the fact that this mode mixture corresponds to the fundamental mode of a circular corrugated waveguide, the HE_{11} mode. This technique reported in [1,5-7] involves a gradual matching of the smooth circular guide to another corrugated one wherein the corrugation depth is smoothly tapered from *$\lambda/2$ to $\lambda/4$*. These two outlined techniques are combined in the so-called radially corrugated horn antennas with a matching device at their input port. In principle, corrugated horn antennas present a wider frequency response than Potter type horns. Their design parameters are basically: corrugation parameters (period, duty cycle, depth, shape, etc...); length and profile of the *$\lambda/2$-to-$\lambda/4$* impedance matching transformer; and the horn geometry in order to optimise the global performance of the horn. In the past, many of the applications involving high performance horn antennas have been equipped with radially corrugated horn antennas. Radially corrugated horn

antennas are one of the best possibilities to accomplish very high radiation pattern requirements and they have been extensively used at mm-wave radiation applications with the only drawback of their difficulty of manufacture as the frequency increases.

The most common radially corrugated horns are the ones where the tapering of the horn is a constant slope. In this type of horns the intention is to generate the HE_{11} fundamental hybrid mode inside the corrugated waveguide and to guide it smoothly to a certain aperture diameter. This type of horns avoided the coupling to any other hybrid mode because the designer thought that the rest of hybrid modes would ruin the radiation pattern. But every horn designer knows now-a-days that this is not completely true since the addition of HE_{1n} modes doesn't affect to crosspolar level but can improve the main beam radiation pattern lowering the sidelobes and helping to improve the Gaussian efficiency in the final radiation pattern, EH_{1n} hybrid modes must be avoided in any case since they add a lot of crosspolar radiation (see Fig. 4.3). Radially profiled corrugated feed horn antennas that improve the radiation pattern by means of optimization of their profile will be presented in the next section. In this section, as a simpler way to understand corrugated horns, the design of the ones that have a constant slope tapering is being covered.

To design a radially corrugated horn antenna for a specific application, the first thing we must define are the corrugation parameters. Such parameters are frequency related are can be chosen according to the corrugated waveguide (see Fig. 4.1) as follows:

- Input radius, R, must be of enough size to allow TE_{11} circular waveguide mode to be above cutoff at the lowest usable frequency and as small as possible to be in monomode operation at the highest cutoff frequency. Sometimes this second condition cannot be met and the TM_{01} mode could be present at the input radius. This aspect is usually defined by the reflection coefficient requirement we must achieve since bigger input radius facilitate this parameter.
- The corrugation depth, d, should be around $\lambda/4$ with λ de free space wavelength at the central frequency (if there are several bands use the central frequency between although such frequency is not considered). This is a parameter to be optimized for every corrugation, so begin with a number around this $\lambda/4$ mentioned.
- The corrugation period, p, should be around $\lambda/3$ with λ the lowest frequency. Use a value rounded to the smallest integer in mm or use at least only one decimal value. The corrugation period is constant along all the corrugated horn, if its dimension is optimized it complicates a lot the fabrication.
- The corrugation tooth width, w, should be around in between $p/2$ to $p/5$ with p the corrugation period frequency. Use a value rounded to the nearest integer in mm or use at least only one decimal value. As thinner the corrugation tooth width, as lower the weight of the corrugated horn, but too thin values complicate a lot the fabrication, don`t use values lower than 0.4 mm for this parameter if you plan to manufacture the mm-wave corrugated horn with a lathe. The corrugation tooth width is also a constant along all the corrugated horn, if its dimension is optimized it complicates a lot the fabrication.

Once the corrugation parameters have been decided, the corrugated horn profile must be prepared. This preparation can be divided in two parts, throat region and flare region:

- The throat region controls the reflection coefficient result mainly. To achieve a nice reflection coefficient for a corrugated horn antenna, the most common technique employed is to adapt the transition between smooth circular waveguide

to corrugated waveguide via a *λ/2* to *λ/4* impedance transformer with consists usually in a taper between *λ/2* and *λ/4* corrugation depths in the first 4 to 10 corrugations, (see Fig. 4.6). As a beginning point use a linear taper in the first 5 corrugations and optimize this tapering for reflection coefficient improvement. The designer must consider that the first corrugation depth cannot be bigger than the input radius because the horn could not be manufactured in one single piece via a lathe. This aspect is in fact the main drawback of this type of corrugated horns.

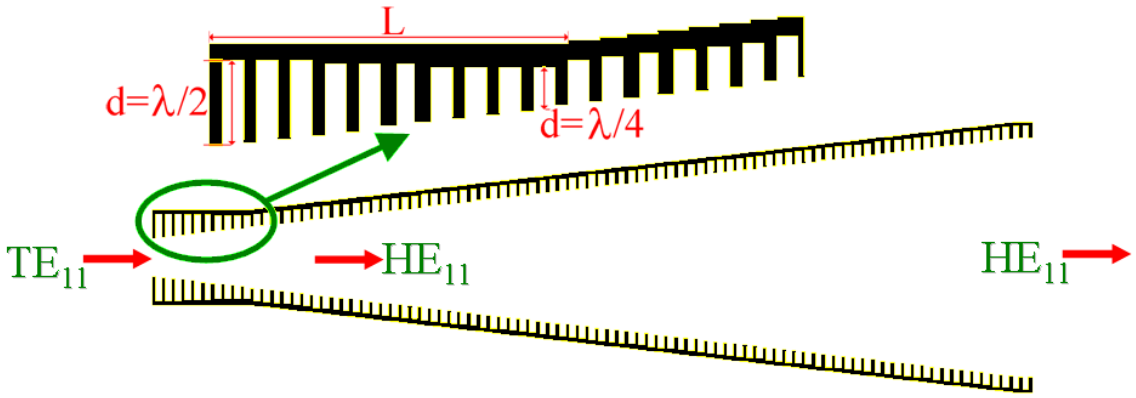

Figure 4.6. Radiation properties of the HE_{11} hybrid mode against aperture diameter (D)

- The flare region, (see Fig. 4.6), controls the radiation parameters. The designer should use as a starting point the diameter given in Fig. 4.7 for a certain directivity. The flare angle selected must be the minimum possible considering the sidelobe level or the spillover power the application can assume. The designer must consider that a low flare angle means longer corrugated horn and more difficult to manufacture, especially as frequency increases.

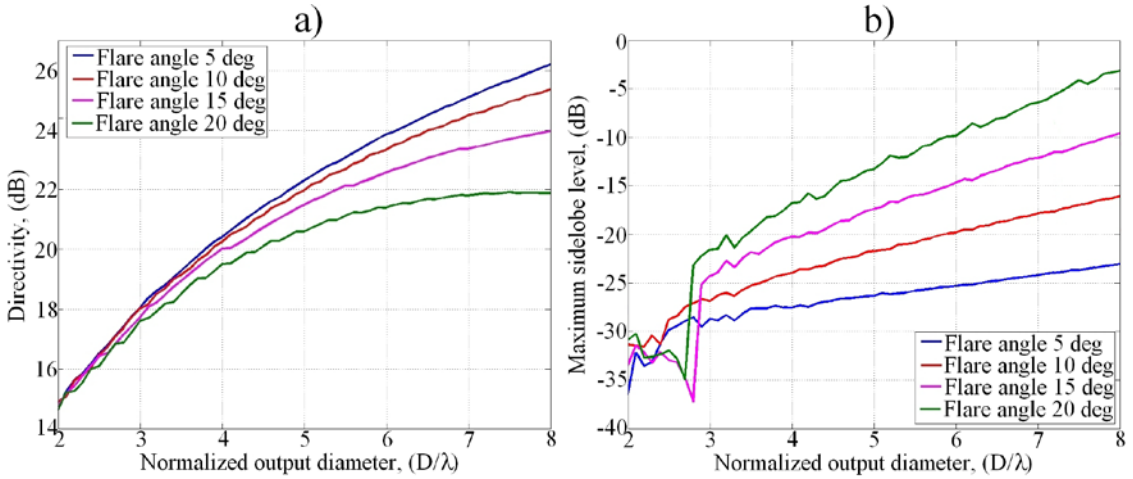

Figure 4.7. a) Directivity design curves for linear taper corrugated feed horns
b) Max. sidelobe level design curves for linear taper corrugated feed horns

As a practical example of how to design a linear taper corrugated feed horn, let's say that we want to design a 22 dB directivity corrugated horn antenna with sidelobes lower than –25 dB and as low return loss and crosspolar level as possible in the most compact profile. Analyzing carefully figure 4.7 and by means of a simple optimization via a mode matching software code [8, 9], the result leads to an antenna of 6.6 degrees taper profile with the first corrugation depth of $0.52 \cdot \lambda$ decreasing linearly with an impedance

transformer of $1.9 \cdot \lambda$ long to a corrugation depth for the rest of the antenna of $0.25 \cdot \lambda$, see Fig. 4.8. The corrugation parameters have been selected as $p=\lambda/5$ and $w=p/3$. The resultant length of the profile is $17.8 \cdot \lambda$ and presents a diameter of $4.86 \cdot \lambda$. It is a quite long antenna for 22 dB directivity. This length cannot be shortened if we must have the sidelobe level at –25 dB or less by any method if we maintain the linear taper corrugated profile, but in the next section we will learn that this can be made by means of an optimization of the profile.

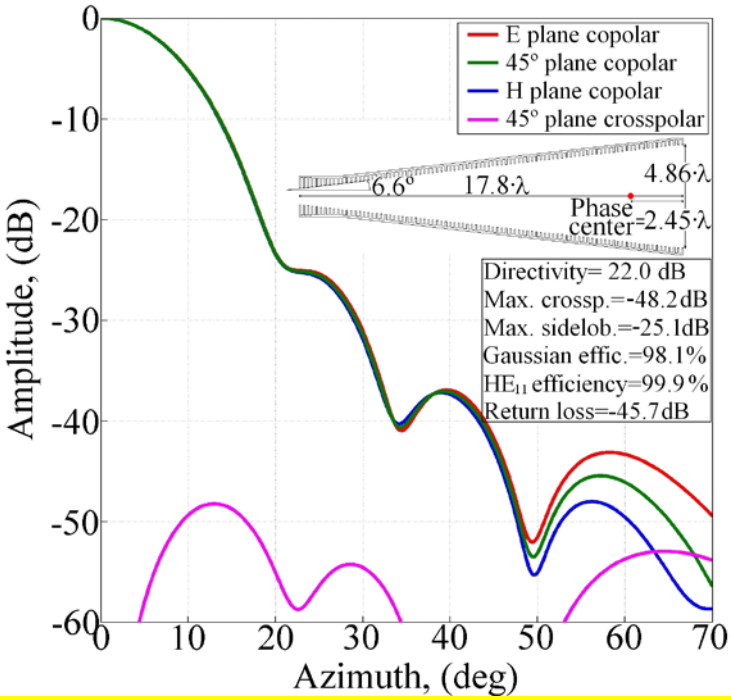

Figure 4.8. Linear taper corrugated horn antenna design for 22 dB directivity and -25 dB maximum sidelobe level

4.2.3 Profiled radially corrugated horn antennas

In the last section, the linear taper corrugated feedhorns have been covered, but there are not much parameters to improve their performance. To overcome the optimization limitations of the linear profiled corrugated horn antennas, during the 90's, several profiles by means of different formulas appeared in the scientific literature. The reason of such formulas was the availability of mode matching techniques (MM) for the design of corrugated horns, but since the computational speed was not too much, the designer should use several formulas to reduce the number of unknowns in the profiled corrugated feedhorn design and increase optimization speed.

A certain number of formulas appeared to solve this problem. In fact, every research group in corrugated horn antennas had their own preferences [10], such formulas were based in square roots, exponentials, sine-squared, polynomials, gaussian, etc. see Fig. 4.9.

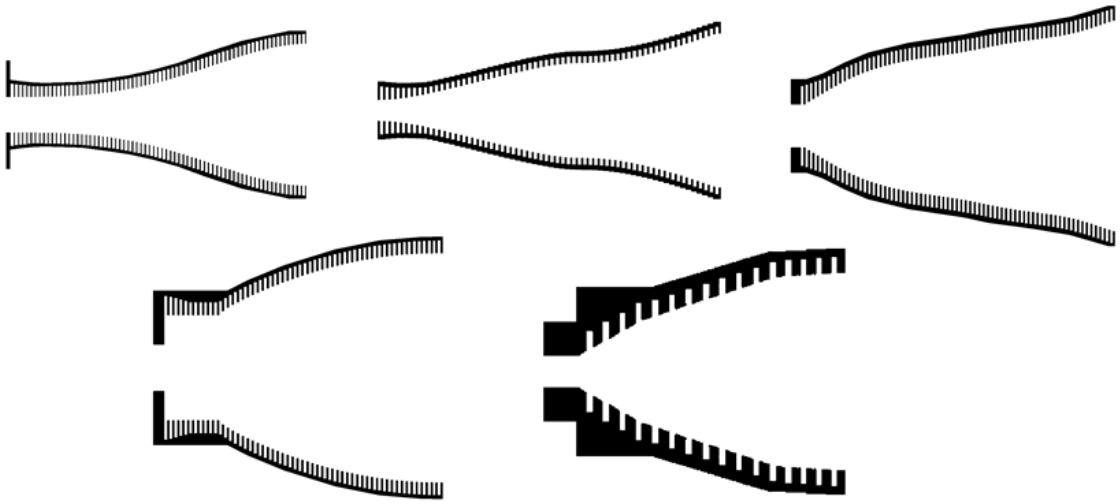

Figure 4.9. Examples of profiled corrugated horn antenna designs

One of the formulas used to profile radially corrugated horn antennas was the gaussian beam expansion formula that is in fact a form of a square root, [11]. This type of formula aroused to implement a perfect match between corrugated waveguide modes (mostly HE_{11} mode or similar mode mixtures) and the fundamental free space modes (fundamental gaussian mode, Ψ_{00}. By using these formula, the matching between the waveguide and the free space was almost perfect, being the most "natural" way to match the two media.

As a practical example of how to design a profiled corrugated feed horn with the profile defined via a gaussian beam expansion formula, let's say that we want to design again a 22 dB directivity corrugated horn antenna but now we are asking for sidelobes lower than –35 dB and as low return loss and crosspolar level as possible in the most compact profile. We use for the profiled radially corrugated feedhorn definition two parts, the first part presents three sections: The first section at the beginning presents a quick and smooth change in the slope at the throat, (less than 10% of the total 1st part length). The second section has a linear taper profile to get quickly to the needed diameter (more than 65% of the total 1st part length). The third section (less than 25% of the total length) is a smoothed end to allow connectivity to the second part corrugated feedhorn profile with a gaussian beam expansion formula, see Fig. 4.10.

Analyzing carefully figure 4.10, the result leads to an antenna of $11.07 \cdot \lambda$ length and $5.64 \cdot \lambda$ aperture diameter. The reduction in length compared to the linear taper profile is a 38% and consider the improved radiation pattern with 10 dB lower sidelobe level, in fact the bigger aperture diameter is caused by such requirement of lower sidelobe level, the same radiation pattern would lead to even shorter solution with the same aperture diameter.

Now-a-days, the availability of optimized mode-matching software packages [8, 9] and the increased speed of computers make possible the optimization of a corrugated feedhorn without the necessity to use a formula that defines the profile. In fact, usually the corrugated feedhorn designers use a formula to define just the initial profile and after that all corrugation radiuses (inner and outer) are optimized individually, so the final appearance of the optimized radially corrugated feedhorn is radically different from any formula and in fact the designer can adapt such optimization to generate the smallest size

possible profiled radially corrugated horn and at the same time comply with all of the stringent requirements usually demanded for this type of feedhorns.

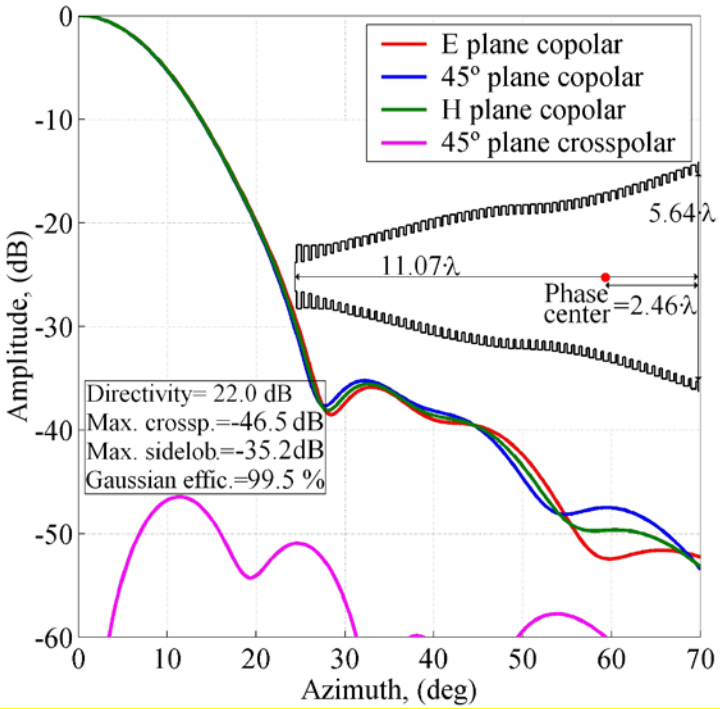

Figure 4.10. Profiled radially corrugated feed horn designed and optimized with a combination of two sections defined by formulas for 22 dB directivity and –35 dB sidelobe level

4.2.4 Corrugated horn antennas that combine axial and radial corrugations

One of the main drawbacks for manufacture of radially corrugated feed horns is the impedance transformer at their throat. This part is difficult to manufacture in a piece by means of a lathe since the farther corrugations are also the deepest and indeed the ones where the fabrication tolerance is worse. This can be solved making such horn in several parts or by making the throat by means of stacked irises but in this section an elegant solution to this problem is being given. This solution not only solves the common manufacture techniques; besides it even results in shortening the total profile by a significant amount.

The solution we are referring to is a horn antenna that combines horizontal corrugations (known also as axial corrugations or choke horns) for the throat region and vertical corrugations (known also as radial corrugations) for the flare region [12]. The design guidelines for this type of corrugated horn antennas were fully explained in [13].

This type of horn antenna achieves significant improvements on the following four parameters, when compared to a normal radially corrugated horn, obtaining the same radiation performance:

1. - Shorter horn axial length
2. - Improved return loss over a wide bandwidth
3. - Smaller computation complexity
4. - Reduction of the manufacturing complexity (avoids the deep first radial corrugations)

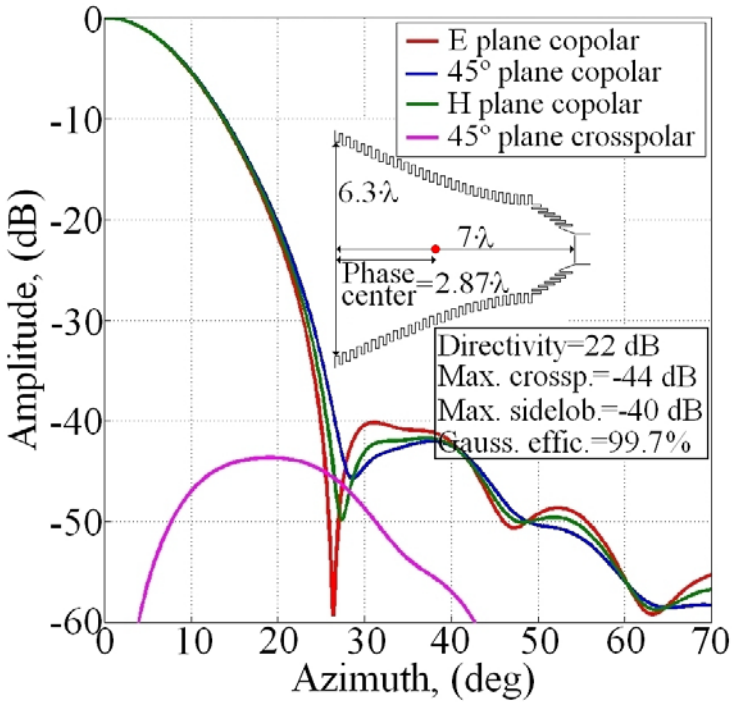

Figure 4.11. Complete corrugated GPHA with a choked corrugated waveguide input for 22 dB directivity and –40 dB sidelobe level

Again, as a practical example of how to design a corrugated horn antenna that combines axial and radial corrugations, let's say that we want also to design a 22 dB directivity corrugated horn antenna but now we are asking for sidelobes lower than –40 dB and as low return loss and crosspolar level as possible in the most compact profile. We use for the throat region an axially corrugated part that presents a linear taper and six axial corrugations. For the flare region, we select a profile defined by a gaussian beam expansion formula, see Fig. 4.11. The solution leads to an antenna of only $7{\cdot}\lambda$ length and $6.3{\cdot}\lambda$ aperture diameter. The reduction in length compared to the optimized radially corrugated profile is a 37% and compared to the linear taper radially corrugated profile the reduction is a 61% and it should also be considered the improved radiation pattern with -40 dB sidelobe level, in fact again the bigger aperture diameter is caused by such requirement of lower sidelobe level, the same radiation pattern would lead to even shorter solution with the same aperture diameter as the previous solutions.

4.2.5 Examples

In this section two examples of advanced corrugated feed horn antennas are being presented. Both have been manufactured at mm-wave frequencies with two different manufacturing techniques and tested obtaining the expected performance simulations predicted.

4.2.5.1 Axial and radial corrugated feed horn antenna design for a mm-wave 80-100 GHz body scanner

An 80-100 GHz corrugated horn design was optimized to act as feed of a rotating reflector for a body scanner. The design was implemented by means of axial and radial corrugations and the main requirement was a very low spillover to achieve as pure as possible image from the body emission at mm-wave frequencies.

The design parameters were a FWHM (Full-Width Half-Maximum) of 14 degrees, gaussian beam decay radiation pattern till 26 degrees in azimuth (view angle from the subreflector) and sidelobes from 26 degrees in azimuth lower than -30 dB. The maximum measured crosspolar level should be below -25 dB and the measured reflection coefficient should be lower than -20 dB.

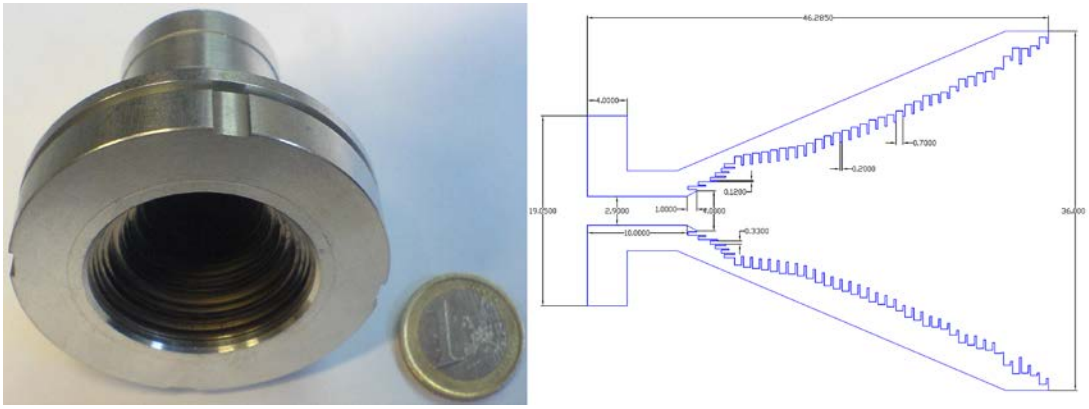

Figure 4.12. Manufactured axial and radial corrugated feed horn antenna design for a mm-wave 80-100 GHz body scanner

The feedhorn was designed with these specifications resulting in a total length of 46.3 mm and an output diameter of 36 mm, (see Fig. 4.12). The manufacture was made by means of iris rings of 0.7 mm and 0.2 mm sequentially stacked to form the radially corrugated part. The axially corrugated part was manufactured with a high precision milling machine.

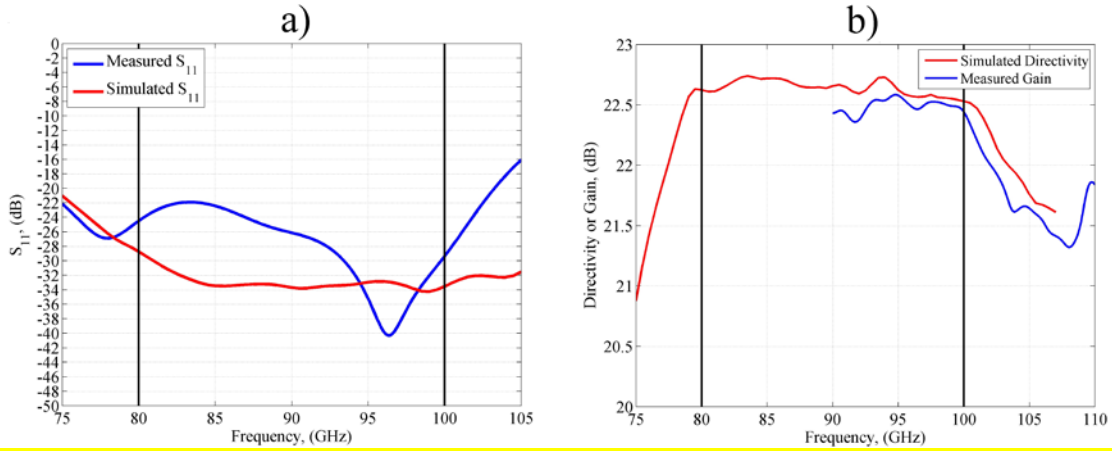

Figure 4.13. Simulated and measured reflection coefficient (a) and gain (b) for the axial and radial corrugated feed horn antenna design for a mm-wave 80-100 GHz body scanner

Simulated and measured reflection coefficient can be seen in figure 4.13a. The measured reflection coefficient is lower than -22 dB in the whole band. Regarding the gain, see Fig. 4.13b, losses lower than 0.2 dB were measured as well. Measured radiation patterns can be checked in figure 4.14, the measured crosspolar level is always below -28 dB for the whole band. The measured main beam radiation pattern decay is as expected from simulations, approximately of 14 degrees FWHM.

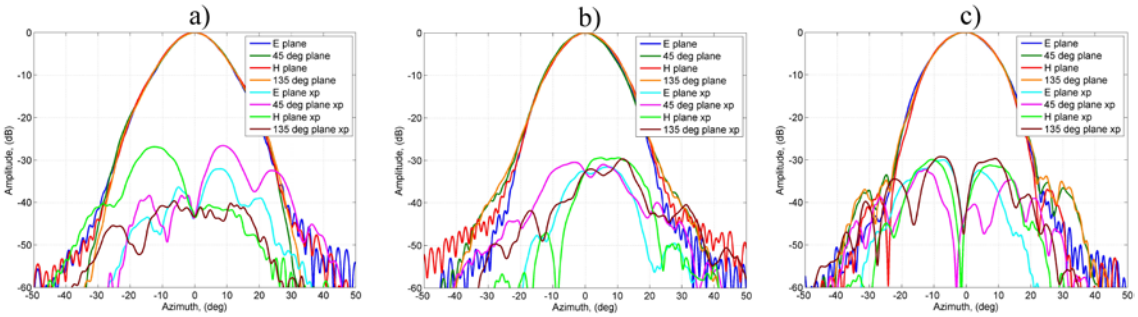

Figure 4.14. Measured radiation patterns at 80 GHz (a), 90 GHz (b) and 100 GHz (c) for the axial and radial corrugated feed horn antenna design for a mm-wave 80-100 GHz body scanner

4.2.5.2 Radially profiled corrugated feedhorns for ESA funded MARSCHALS airborne system

MARSCHALS was a three channel limb sounder for the European Space Agency (ESA) that flew on an aircraft. The designer of the mission were especially concerned about the sidelobes generated by the feedhorns or the rest of the optics. The aim of the MARSCHALS project is the limb observation, and therefore any power introduced via a sidelobe pointing the earth should be consider as noise decreasing the performance of the whole system. The sidelobe requirement was *–35 dB* in both feedhorn designs.

The requirements for these corrugated horn antennas (called antenna in band C and antenna in band D), were the following:

Band	Frequency Range	Centre Frequency	Beamwaist Radius
C	*316.5 - 325.5 GHz*	*321.00 GHz*	*2.078 mm*
D	*342.2 - 348.8 GHz*	*345.50 GHz*	*2.003 mm*

Table 4.2. MARSCHALS feedhorns requirements

Other parameters common to both antennas were the following:

- Sidelobes: It was required sidelobes to be less than -*35dB* (with no "shoulders" on the main lobe). Obviously the lower the better.
- Peak crosspolar: below -*35dB* (again, the lower the better)
- Feed waveguide: Full height rectangular waveguide (*0.762 x 0.381 mm*).
- Horn Length (flange to aperture): Maximum *40 mm*.

The manufacture of the complete corrugated feed horn was made by means of high precision electroforming including the rectangular to circular transition to the rectangular feed waveguide of *0.762 x 0.381 mm* dimension. To reduce the manufacture complexity, the corrugation tooth width should be exactly half of the corrugation period and constant along the whole antenna.

The bandwidth requirements were not too tight, *2.8%* for the C band antenna and 1.9% for the D band antenna. The resultant directivity, by means of translation of the beamwaist radius values of table 4.2, was quite high; *2.078 mm* beamwaist radius at *321 GHz* in C band antenna means an illumination at *16 degrees* of *–35 dB* and therefore a directivity of *26 dB*. As well, the *2.003 mm* beamwaist radius at *345.5 GHz* in D band antenna means an illumination at *15.5 degrees* of *–35 dB* and therefore a directivity of *26.3 dB*.

The transition from rectangular to circular waveguide was designed ending in a circular diameter of *0.762 mm*. This diameter was used as the input waveguide diameter for both antennas. After the optimisation of both profiles, these were the results:

- The total length of the C band antenna is *39.1 mm* (*41.9·λ*) and the output diameter *8.29·λ* (*7.74 mm*). A picture of the antenna is shown in figure 4.15a.
- The total length of the D band antenna is *39.1 mm* (*45.1·λ*) and the output diameter *8.53·λ* (*7.398 mm*). A picture of the antenna is shown in figure 4.15b.

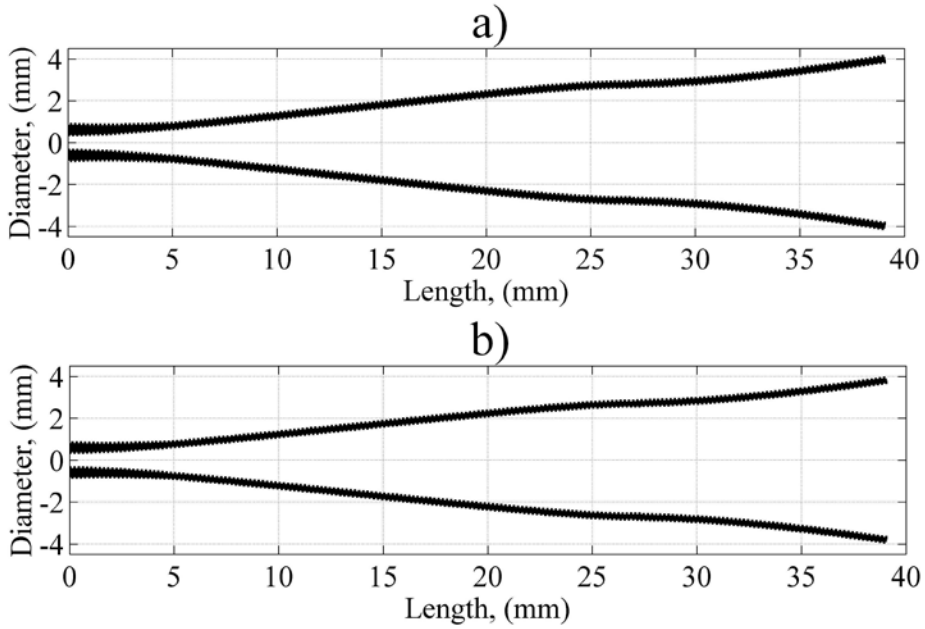

Figure 4.15. a) MARSCHALS feedhorn proposed profile for C band
b) MARSCHALS feedhorn proposed profile for D band

The rectangular to circular transition design was very simple and it was a direct cut of *15 degrees* angle of the circular input waveguide of each antenna in a *0.711 mm* length to result in the *0.762 x 0.381 mm* input rectangular waveguide, (see figure 4.16).

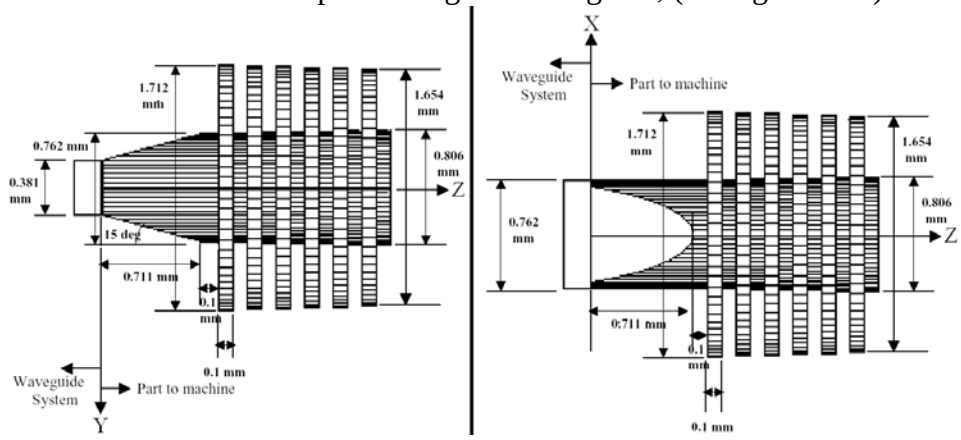

Figure 4.16. MARSCHALS feedhorns throat region with rectangular to circular transition

The antenna was manufactured using an electroforming technique. Electroforming is a metal forming process that forms parts through electrodeposition or electroplating on a model, known in the industry as a mandrel. The mandrel was made by a milling machine and a picture of it can be seen in figure 4.17. Metallic mandrels are pre-treated chemically to allow subsequent separation of the finished electroform. The outer surface of the

mandrel forms the inner surface of the form. A thick layer of electroplating copper is applied until the plate itself is strong enough to be self-supporting. The mandrel is dissolved away after forming. The surface of the finished part that was in intimate contact with the mandrel is rendered in fine detail with respect to the original, and is not subject to the shrinkage that would normally be experienced in a foundry cast metal object, or the tool marks of a milled part. It can be observed in such figure 4.17 the extremely high precision manufacturing of the mandrel remembering that the corrugation tooth width is only *0.1 mm*.

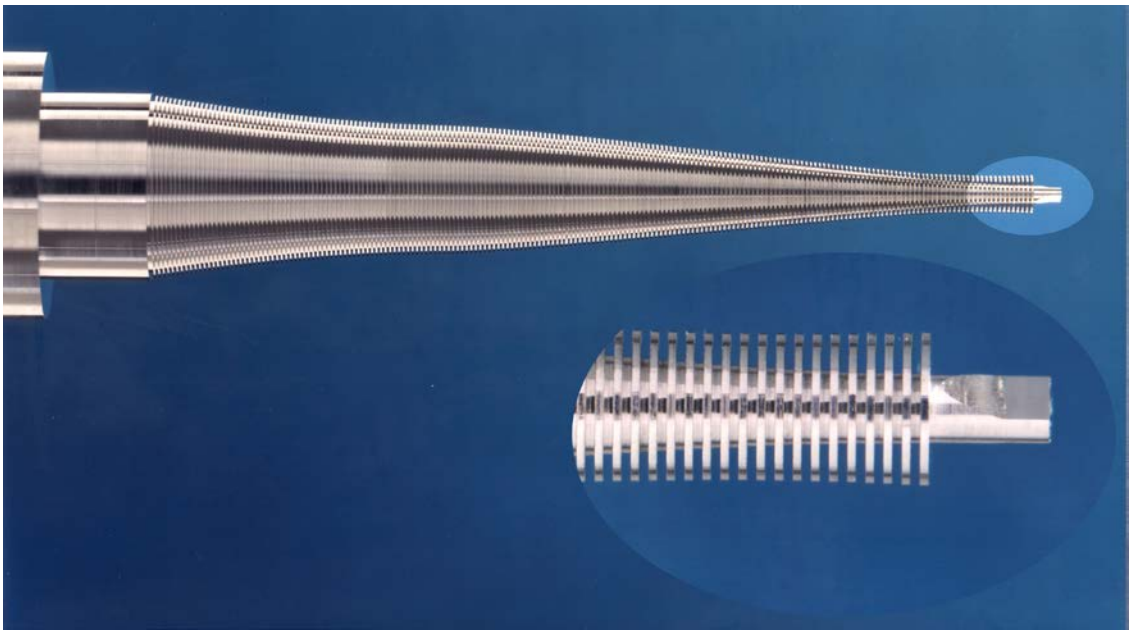

Figure 4.17. Mandrel of one of the MARSCHALS feedhorns

Simulated results for both antennas at central frequency can be found in Figs. 4.18 and 4.19. Both antennas meet all the specifications widely.

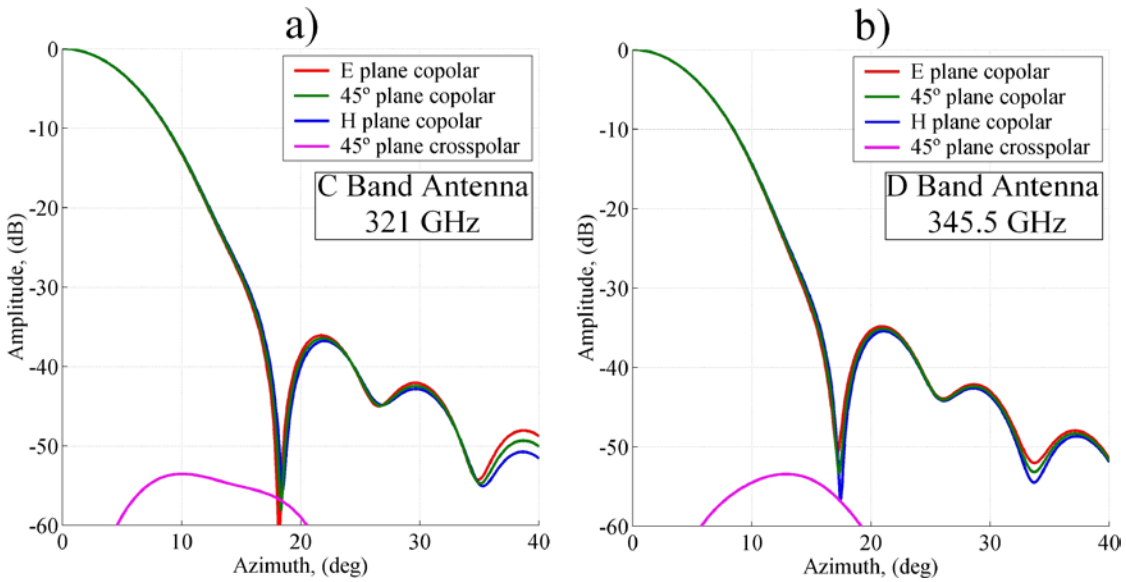

Figure 4.18. Simulated far field radiation pattern of both MARSCHALS feedhorns

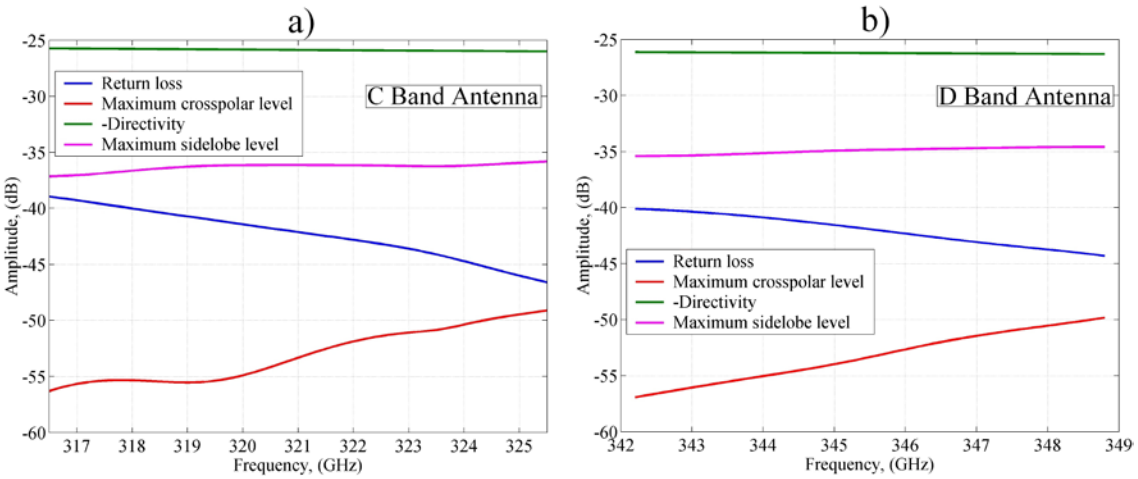

Figure 4.19. Simulated far field behaviour of both MARSCHALS feedhorns

4.3 Smooth walled feed horns

This section describes the technology concerning the smooth walled feed horn technology for mm-wave and submm-wave frequencies. It begins with a short introduction to smooth walled feed horn profiles and continues with the main techniques to design this type of feed horns, multi-flare angle and spline profiled.

This type of horns present worse radiation characteristics compared to corrugated profiled ones and are much longer. However, these are much simpler and cheaper to manufacture at high frequencies, so many times are the preferred choice. This problem regarding manufacture of corrugated horns at frequencies above 100 GHz becomes particularly acute when many tens, hundreds or even thousands of horns are required for large format focal plane array receivers. Therefore, there has been much recent interest in the use of easy-to-fabricate smooth walled horns [14] at these shorter wavelengths.

4.3.1 Introduction to smooth walled feed horn profiles

Typically, smooth walled horns either have step or flare angle discontinuities, or smoothly varying interior profiles. The shapes of the horn interiors are optimized numerically by mode matching techniques [8, 9] to generate a balance of higher order waveguide modes which leads to a uniform aperture illumination and hence far-field patterns with high beam circularity, low sidelobe levels and low crosspolarization.

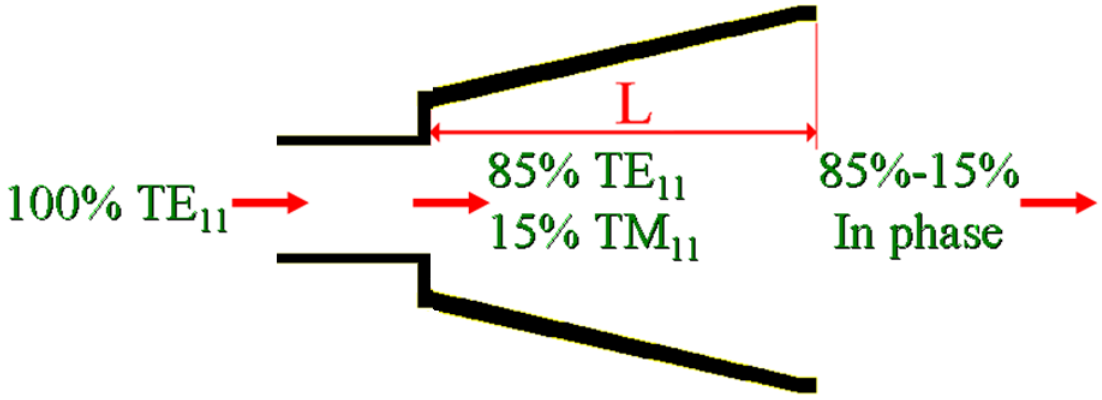

Figure 4.20. Principle of operation of a Potter type horn

The simplest form of a smooth-walled horn is a Potter type horn [15], which has only one step discontinuity near the throat followed by a conical flaring section, (see Fig. 4.20). The step discontinuity excites the TM_{11} mode at about 15% of the total incident power of the incoming TE_{11} mode. Both fields propagate along the conical flaring section until they arrive in phase at the horn aperture.

Figure 4.21 shows the electric field of the TE_{11} and TM_{11} modes, and it can be seen clearly that the addition of both in the correct proportion and in phase produces a linearly polarized electric field at the aperture of the horn. The combination of 85% of TE_{11} and 15% of TM_{11} leads in fact to an HE_{11} hybrid waveguide mode, (see Table 4.1), being the mode mixture that generates automatically a linear taper corrugated horn. As it was indicated in the section regarding corrugated horns, this mode combination generates a highly uniform field that produces a radiation pattern with low sidelobes level and low cross-polarization approximating to the performance of a corrugated feed horn. But the main disadvantage of the Potter horn is that it has a narrow operating bandwidth (5 to 8%).

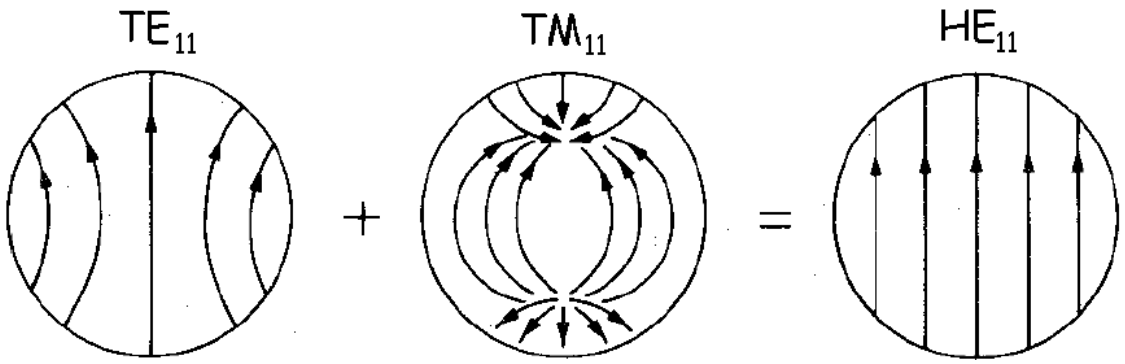

Figure 4.21. Combination of modes pursued in a Potter type horn

However, the performance of a Potter type horn can be substantially improved by increasing the number of discontinuities of the horn. These types of horns are known now-a-days as multi-flare angle feed horns [16] and are being covered in the following section. On the other hand, there is another method of optimizing a smooth walled feed horn profile with even better results, this method consists in the optimization of the coefficients of a spline curve to meet the specific radiation parameters needed for a certain application [14], these types of horns will be covered in the next to the following section.

4.3.2 Smooth walled multi-flare angle feed horns

The Potter type horn antenna exhibits nice radiation properties, but in a reduced bandwidth. To improve the performance the designer increasing the number of discontinuities of the horn. With some more parameters to optimize, the designer can generate a carefully chosen combination of the higher order modes which could widen the operating bandwidth of the horn and maintain the nice radiation properties.

The simplest multi-flare angle horn is the Turrin type horn [17], see Fig. 4.22. This type of horn starts with a short conical section with a cone angle and then is followed by another conical section of lower angle.

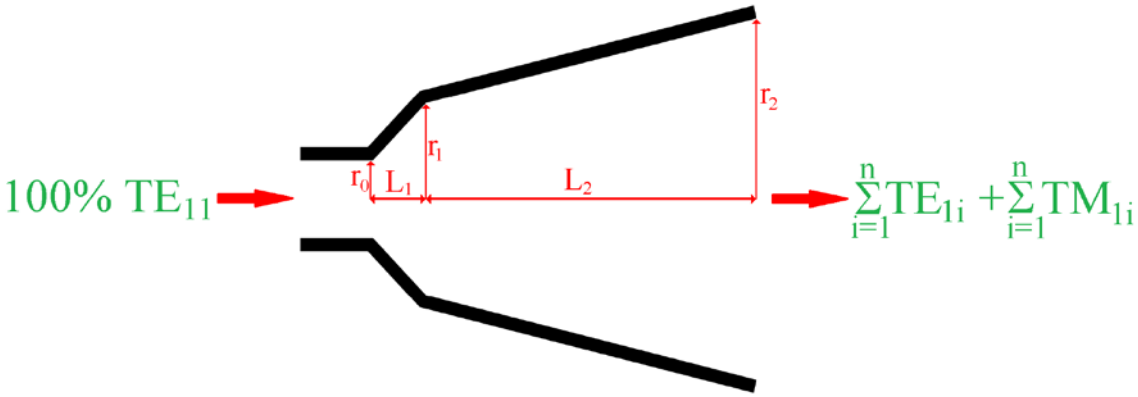

Figure 4.22. Principle of operation of a Turrin type horn

After the Turrin type horn that only has two different angles, (see Fig. 4.22), the designer can add as many discontinuities in the throat region of the horn as he needs, these types of horns are then known as multi-flare angle horns, (see Fig. 4.23). The optimized depth of these discontinuities (R_0, R_1, R_2, R_3…), the horn length and flare angles (L_1, L_2, L_3…), can be predicted using modal matching in conjunction with optimization algorithms to derive the desired radiation properties in a certain bandwidth.

Step or flare-angle discontinuities near the throat of the horn will, unavoidably, excite other higher modes (TE_{1n} and TM_{1n}) in addition to the desired TM_{11} mode. These higher order modes will affect the aperture field in a complicated, frequency dependent way, making the design of multi-flare angle horns that give good performance over a finite bandwidth more difficult. Fortunately, the effect of these modes on the far-field pattern of a particular horn can be predicted very accurately using the numerical modal-matching techniques. Since such modal matching techniques can be used to calculate the far-field patterns, it is possible also to use this technique in conjunction with suitable optimization algorithms to determine the optimum horn profiles for good performance over a particular bandwidth, [7, 8].

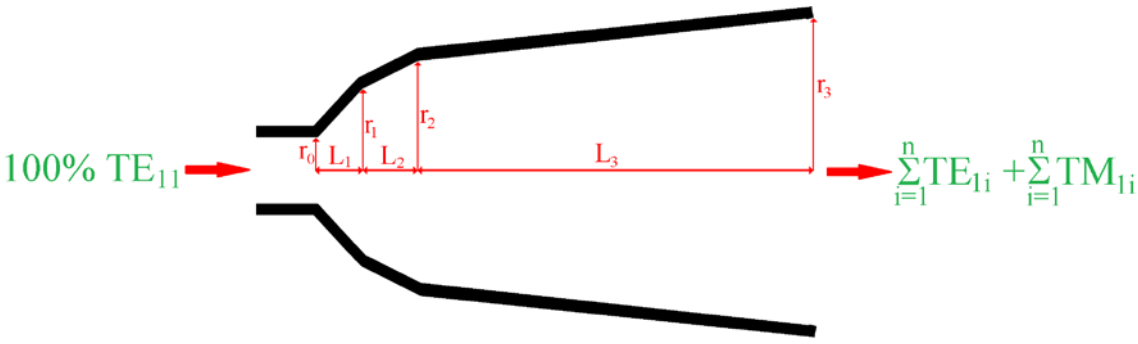

Figure 4.23. Multi-flare angle smooth waveguide feed horn with three steps

These types of horns are very suitable for manufacture at mm-wave and submm-wave frequencies since they can be made very quickly and cheaply by repeated drilling with a properly shaped electrode as machine tool, [18] or even by additive manufacturing techniques with a certain post processing of the manufactured result. In figure 4.24, a set of four feed multi-flare angle smooth walled feed horns for a communication system at 330 GHz is presented. Such submm-wave horn array was manufactured by means of an

additive manufacturing technique called direct metallic laser sintering, the array needed a postprocessing with properly shaped electrode to be fully functional.

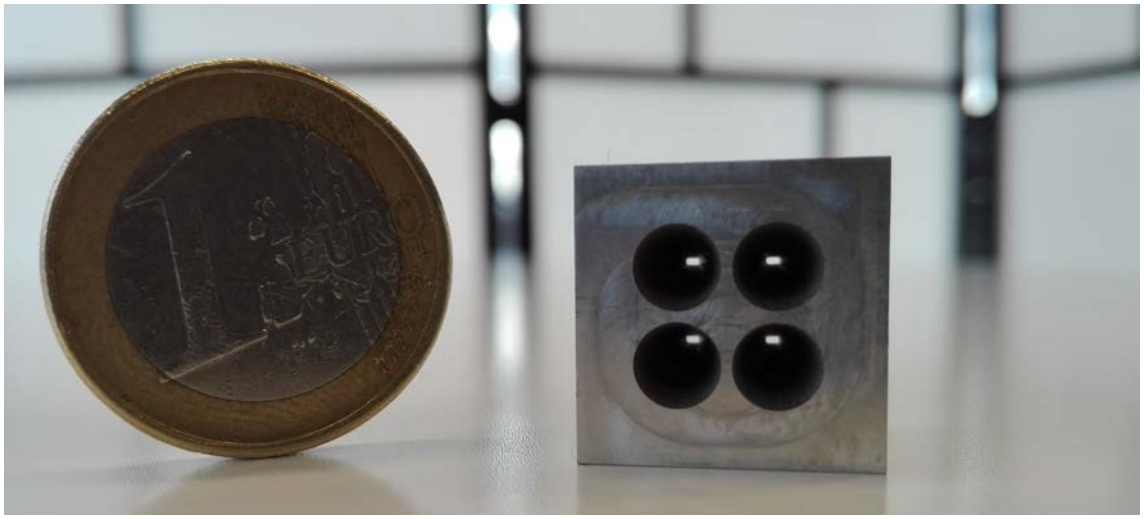

Figure 4.24. Direct metallic laser sintering manufactured 2x2 antenna array of multi-flared angle smooth walled feed horns for a communications system working at 330 GHz (courtesy of ANTERAL S.L.)

4.3.3 Smooth walled spline profiled feed horns

The smooth walled profiles defined in the previous section are formed by steps, but it could be interesting to have the possibility to design a smooth walled profile whose taper is smoothly opening without any discontinuity. To fill this gap in 2004 the researchers from CSIRO in Australia presented their contribution, and they called it the smooth walled spline profile [14]. This profile was developed as a substitute of corrugated horns for mm-wave and submm-wave frequencies since the manufacturing complexity is much reduced. Their performance is not as good as a corrugated horn but it is quite acceptable considering and bandwidth around 30 % can be easily achieved for crosspolar levels below -30 dB. In fact, in many cases (as feed for multibeam reflector antennas) smooth walled spline profiled feed horns have replaced corrugated horns for onboard satellite payload [19].

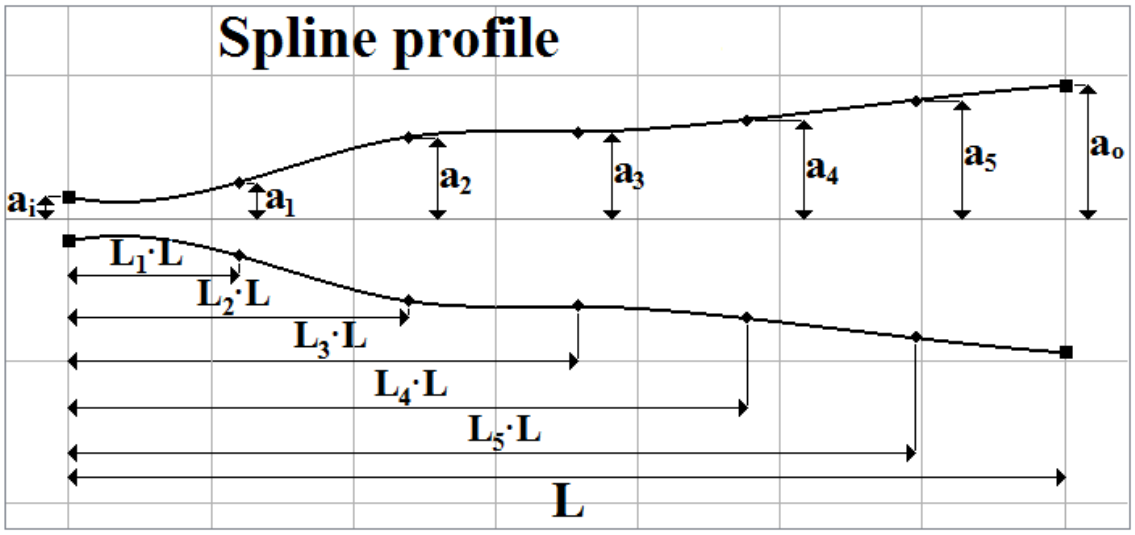

Figure 4.25. Spline profile feed horn geometry [14]

The spline profile is a numeric function that is piecewise-defined by polynomial functions and which possesses a high degree of smoothness at the places where the polynomial pieces connect, see Fig 4.25. In fact, the term spline was adopted from the name of a flexible strip of metal commonly used by drafters to assist in drawing curved lines.

To design a smooth walled spline profile feed horn antenna for a specific application, we must define first the initial dimensions of the horn we want to develop. We need as an initial approach three parameters: input radius, output aperture radius and total length. Once they are defined we should decide how many optimization points we need. Many optimization points will allow a better result, but the optimization time will be longer; a few optimization points (in the Fig. 4.25 only five variables are used) allow a quicker optimization time, but perhaps they are not enough to reach the requirements needed.

If the designer need to achieve a better result, he must increase the number of optimization radiuses, in fact in [20] the authors increase the number of optimizable radiuses till 20 unknowns improved the result significantly.

As an example, a K/Ka band smooth walled spline profile feed horn for a communications satellite is presented, see Fig. 4.26.

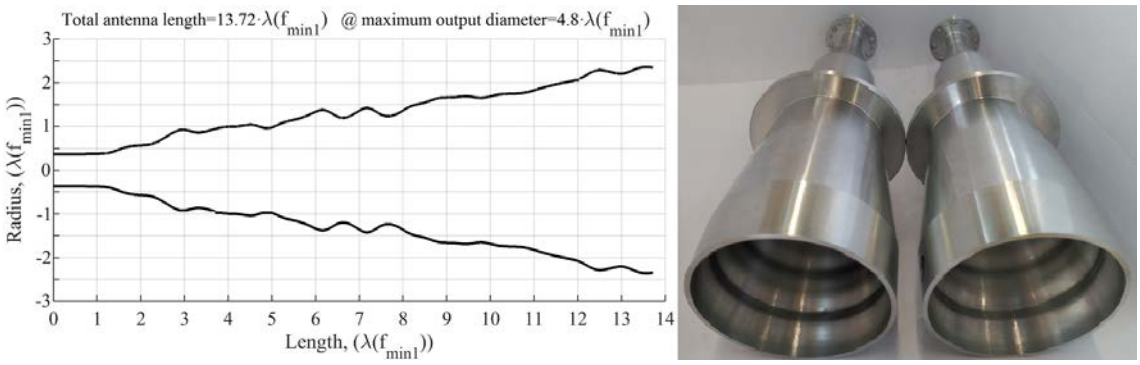

Figure 4.26. Optimized smooth walled spline profile feed horn for onboard a communications satellite (courtesy of ANTERAL S.L.)

Such a feed horn has more than a 42.3% bandwidth and the partial bandwidths were 3.5% and 2.4%. Therefore, it is a wideband design and its requirements are extremely severe for a smooth walled horn, since a return loss value better than 40 dB and a crosspolar level below -26 dB were required for both frequency bands, and they are quite apart in frequency. In addition, it is very short for a spline profile.

The design employs 40 radiuses to define the profile (see Fig.4.26). The outcome is that of a rather curved inside for smooth walled horn, but the results (see Figs. 4.27 and 4.28) show that the requirements are met.

The resulting radiation patterns can be seen in Fig. 4.28. This horn antenna was manufactured and is successfully operating onboard a geostationary satellite, where it is part of a feed horn array for spot beam communications.

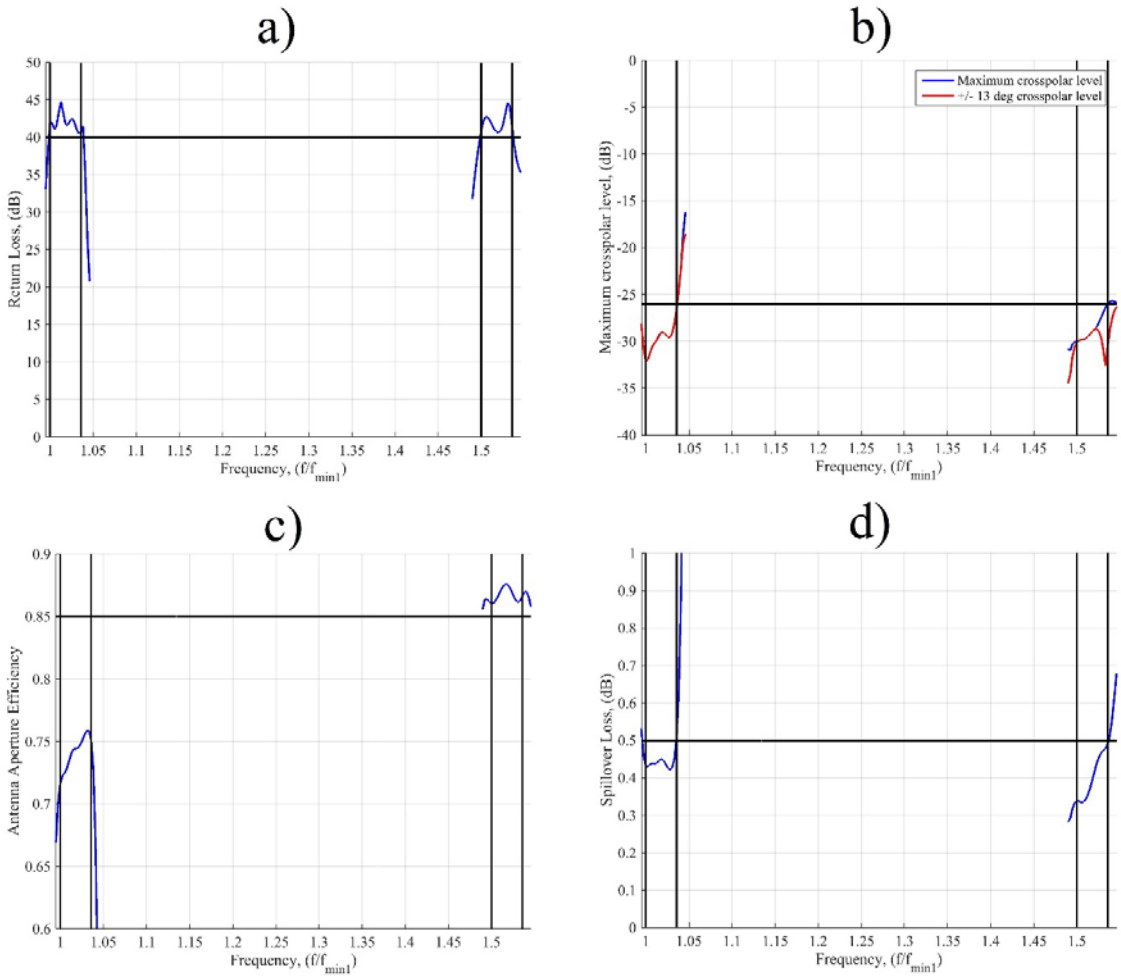

Figure 4.27. Results of the optimized smooth walled spline profile:
a) Return loss b) Crosspolar level
c) Aperture efficiency d) Spillover loss above 13 degrees

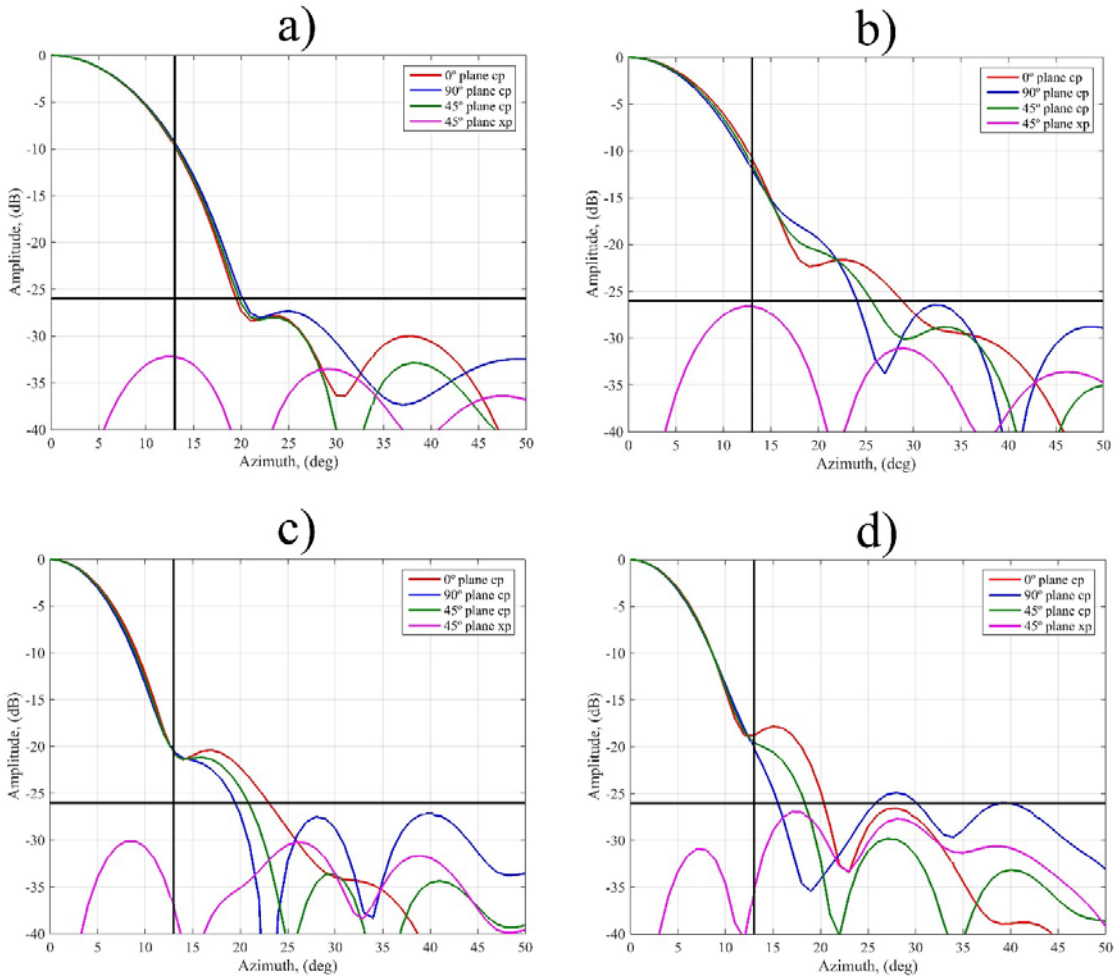

Figure 4.28. Far field radiation patterns of the optimized smooth walled spline profile: a) At f_{min1} b) At 1.04·f_{min1} c) At 1.5·f_{min1} d) At 1.54·f_{min1}

4.4 Metamaterial based feeds

This section describes different feed configurations based on metamaterial structures. The field of metamaterials is very broad and several examples of metamaterial based or inspired antennas are considered along this book. In this case metamaterial antennas, which resemble or create horn like antennas are treated. First the metallic walls of the horns will be substituted by a tailored surface so that different properties are achieved. These antennas are based on the so-called hard and soft surfaces, which can be considered as special cases of metasurfaces. Finally, horn antennas will be constructed based on 3D electromagnetic bandgap (EBG) structures. Their fundamentals and several examples are given in the following sections.

4.4.1 Soft and hard horns

Corrugated horn antennas can be considered as a particular case of the more general concept of hybrid mode horns [21]. These antennas support linear polarized modes

provided than an anisotropic boundary condition exists in the horn walls. The condition to be fulfilled by the boundary impedances is called balanced hybrid condition:

$$Z_{TE}Z_{TM} = \eta_0^2$$

where Z_{TE} and Z_{TM} are the TE and TM boundary impedances and η_0 is the free-space wave impedance.

Two families of antennas satisfy this condition, leading to the so-called hard and soft horns [21]. In the soft horn case the boundary conditions correspond to:

$$Z^{TE} = Z_x = \frac{E_x}{H_z} = 0$$

$$Z^{TM} = Z_z = \frac{E_z}{H_x} = \infty$$

Whereas in the hard horn they are:

$$Z^{TE} = Z_x = \frac{E_x}{H_z} = \infty$$

$$Z^{TM} = Z_z = \frac{E_z}{H_x} = 0$$

Soft horns support tapered aperture distributions which lead to very low side lobe radiation patterns. Conversely, hard horns provide uniform aperture distributions which correspond to very high aperture efficiencies.

These hybrid mode horns have been implemented with different techniques, which are reviewed in [22]. These include longitudinal and transversal corrugated horns, dielcore horns, strip loaded and metamaterial or metasurface wall horns. This last case constitutes the most novel implementation and, thanks to the flexibility of metamaterials a very promising alternative to the conventional implementations. The following section describes different implementations of these concepts.

4.4.2 Metamaterial horns

Metamaterial based horn antennas, as schematically shown in Fig. 4.29, can be employed for alternative implementations of the dielcore horn designs. Since metamaterials allow obtaining values of the dielectric constant lower than 1, both hard and soft surface designs can be constructed based on the dual dielcore horn. In both cases the core dielectric can be taken as air, which requires the outer dielectric to have dielectric constant lower than 1, which can be achieved by a metamaterial. This has additional advantages, since removing the central core allows reducing mass and losses and improves reflections in the interface between the air-filled feeding waveguide and the dielectric loaded horn antenna.

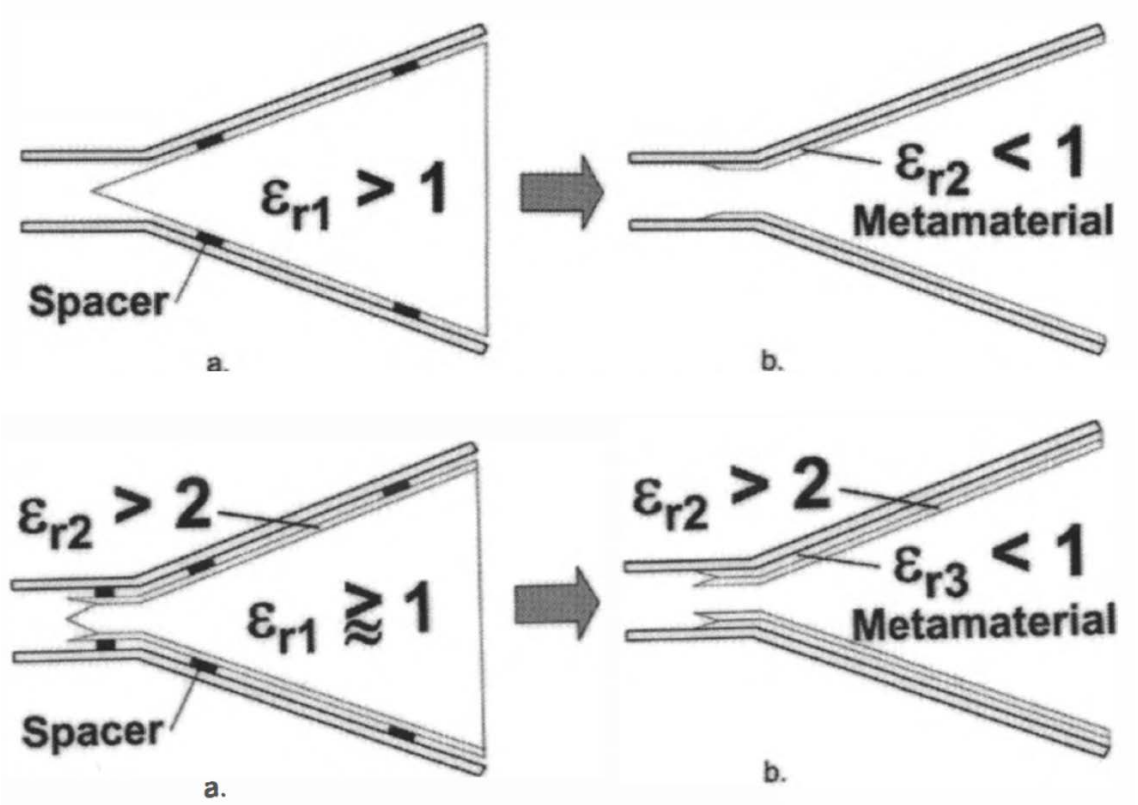

Figure 4.29. Schematic of hard and soft antenna implementations using metamaterials as alternatives to the dual dielcore horns [22].

The concept behind these antennas was first demonstrated by [22]. Simulation results showed that the performance of these antennas complied with the expectations. However, the results were based on theoretical materials with ideal parameters.

The challenge of finding a metamaterial realization which complied with the required parameters was sorted out by [22]. The developed metamaterial is based on a wire grid with wires in the three coordinate axis directions, so that the structural elements of the metamaterial affect all the field components and full control of the surface impedance can be achieved. The first experimental demonstration of a horn antenna based on this metamaterial wall was carried out by the same group [23]. A photograph of the manufactured antenna is shown in Fig. 4.30a. The achieved pattern was symmetric, with low sidelobes along the full super-extended C-band. A comparison between the E-Plane pattern of this antenna and a trifurcated and standard pyramidal horn is presented in Fig. 4.30b. Lower sidelobes than in the conventional counterparts have been achieved by means of the metamaterial surface.

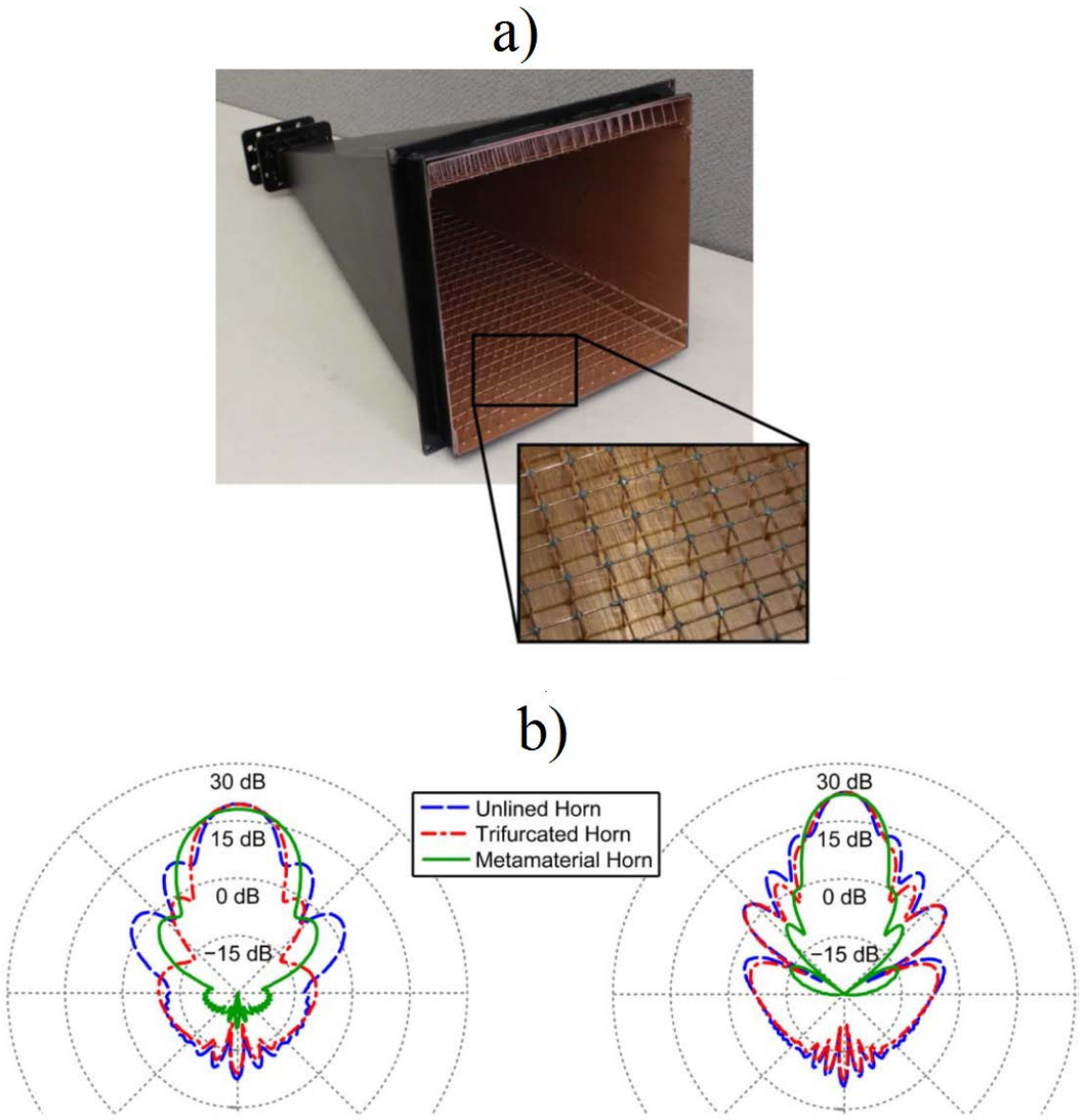

Figure 4.30. a) Photograph of metamaterial horn prototype, with inset showing the wire grid used to create the metamaterial surface.
b) Comparison of the radiation pattern on the metamaterial horn, a standard pyramidal horn and trifurcated horn [23].

In order to simplify the antenna manufacturing a planar metasurface was presented in [24], where a metasurface implemented on a circuit board was used to create a soft horn antenna. Photographs of the prototype are shown in Fig. 4.31. The achieved performance shows sidelobes at the -30dB level, in agreement with the soft nature of the horn. These are nearly 20 dB lower than those obtained with a similar smooth wall pyramidal horn and is maintained in the whole Ku band.

An example of the measured patterns are presented in Fig. 4.31b. Very symmetrical patterns are achieved leading to low crosspolarization levels (around 30 dB).

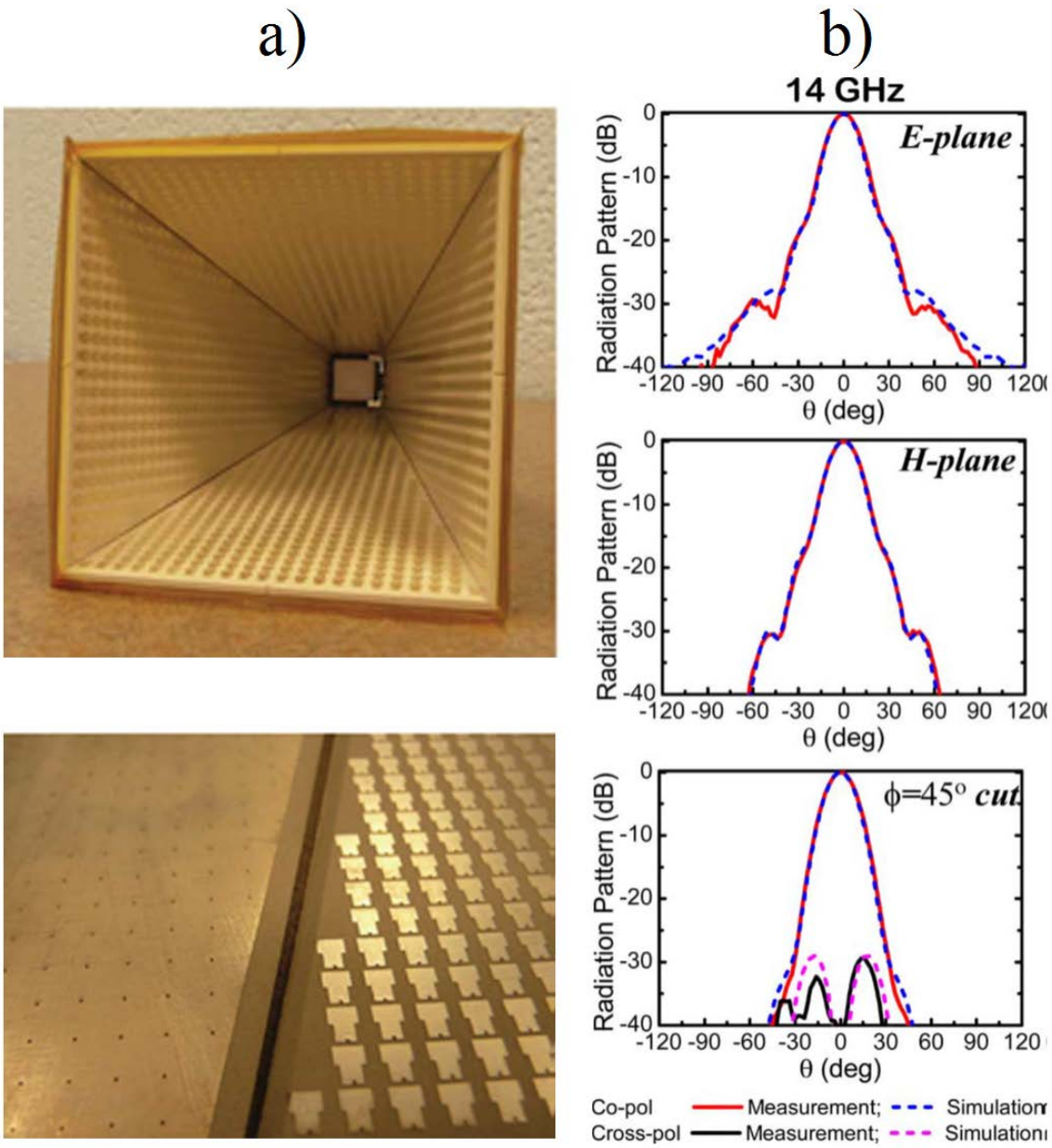

Figure 4.31. a) Photographs of the fabricated metahorn antenna and the metasurface liners on the PCB.
b) Measured and simulated E-plane, H-plane, and $\phi = 45º$ plane cut co and cross-polarized radiation patterns of the metahorn at 14 GHz [24]

One problem associated with these antennas is the need of a matching section to reduce reflections at the interface between the smooth wall and the metamaterial sections of the horn. In this case a dielectric section with an optimized profile is used for this purpose. This requires a brute force optimization which can be avoided if a tapered transition is implemented in the metamaterial wall liner. This approach has been followed in [25]

Finally another implementation of this concept was used in [24], applied to a conical horn antenna. The metasurface was based on a mushroom structure, see fig 4.32.

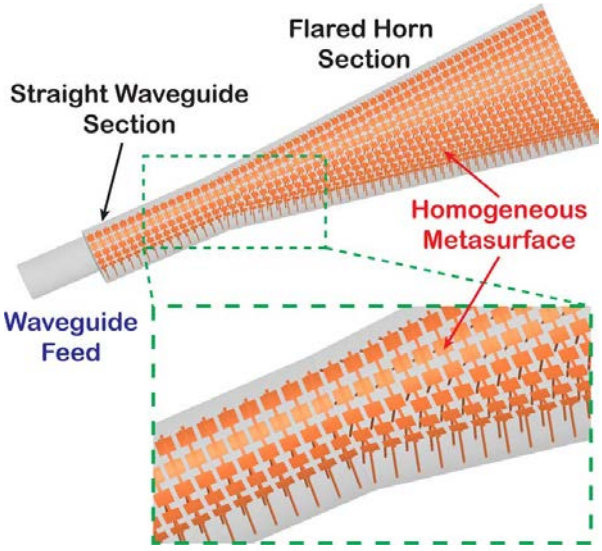

Figure 4.32. Schematic of the conical metamaterial horn antenna proposed in [24]

4.4.3 EBG horn antennas

Electromagnetic band gap materials can be considered as a type of metamaterials. They are 3D periodic arrangements of elements, usually dielectric materials, which, by properly choosing their shape and special position present a frequency range where no propagation of electromagnetic radiation is allowed [26]. This frequency range is called the bandgap and its use has been proposed to reduce the effect of surface waves in planar antennas [27]. This effect can be obtained with planar configurations, usually based on printed board technologies or with 3D structures, where the material must be tailored in three dimensions.

In this last case, if defects are created in the otherwise perfect periodic structure, cavities and waveguides can be created. These can be considered as linear defects and their performance is similar to that of metallic waveguides. Therefore, the same techniques that are used in order to create horn antennas can also be applied in this case.

Horn-like structures have been proposed based on 2D and 3D EBG structures [28]. However, we will focus on those horn configurations based on 3D EBG structures. Among them, the most used EBG for these experiments is the woodpile or layer-by-layer structure [29, 30], due to its simplicity and relatively easy manufacturing up to the submillimetre wave range [31, 32]. As a matter of fact, it is in these high frequency ranges where this type of configurations can be of interest thanks to their low losses due to the absence of metals (provided the EBG structure is fabricated with sufficient precision).

4.4.4 Sectoral horn antennas

The simplest way to create a horn antenna based on a woodpile structure is by altering the bars of one of its layers. Removing one bar will create a waveguide and by tilting those bars that form the waveguide walls sectoral antenna is created. Given the polarization of the mode in the woodpile feeding waveguide this antenna corresponds to a H-plane sectoral horn. The radiation properties of the antenna depend on the flare angle and the antenna length, as in standard metallic sectoral horns.

These configurations were first studied by Weily et al. [33]. An example of the radiation pattern achieved can be seen in Fig. 4.33b. It is worth noting the non-symmetric E-Place cut, due to the asymmetry of the woodpile in the stacking direction. Moreover, given the adiabatic nature of the transition, good impedance matching was achieved between the EBG waveguide section and the horn. In [34] the same group proposed a transition between rectangular and EBG waveguides, with good performance. This configuration was employed to create an array of such antennas with which scanning performance was demonstrated. The radiation pattern of the 16-element array for different scanning angles is shown in fig. 4.33c.

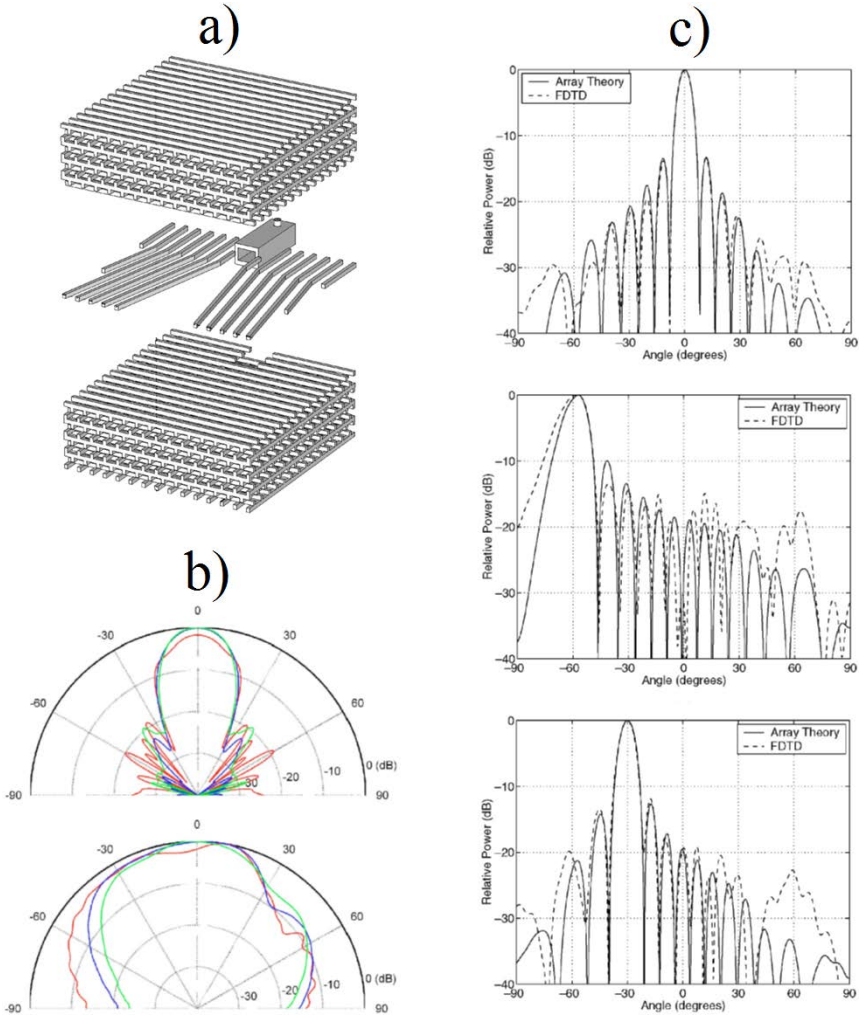

Figure 4.33. a) Perspective view of the woodpile EBG sectoral horn antenna. [34]
b) Radiation pattern
c) Array theory and FDTD computed E-plane radiation patterns for the 16-element linear array for scan angles of: (a) 0º, (b) 60º, (c) 30º

4.4.5 Evanescently fed EBG horn antenna arrays

Another way of controlling the radiation E-plane is by arraying two sectoral EBG antennas. They can be simultaneously fed by means of the so-called evanescent coupling method [35]. In this configuration, an EBG waveguide is used to couple the two sectoral horns by properly adjusting their relative position, as shown in Fig. 4.34. This way, narrower E-Plane cut can be obtained while maintaining the same H-plane of the individual sectoral antennas, as shown in Fig. 4.35, where the simulated and measured antenna radiation patterns obtained with this antenna are compared.

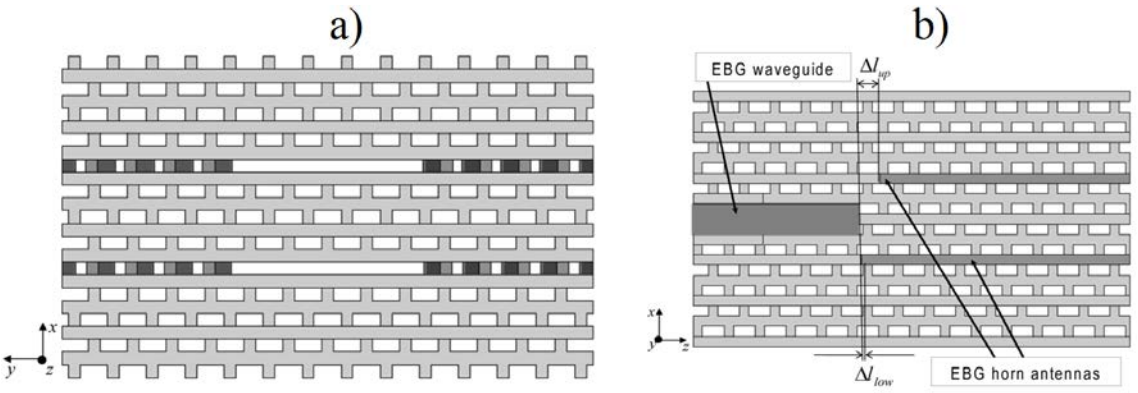

Figure 4.34. Front- and side-view of the evanescently-fed double EBG horn antenna. Dark areas represent the feeding EBG waveguide region and the EBG horn antenna layers [35]

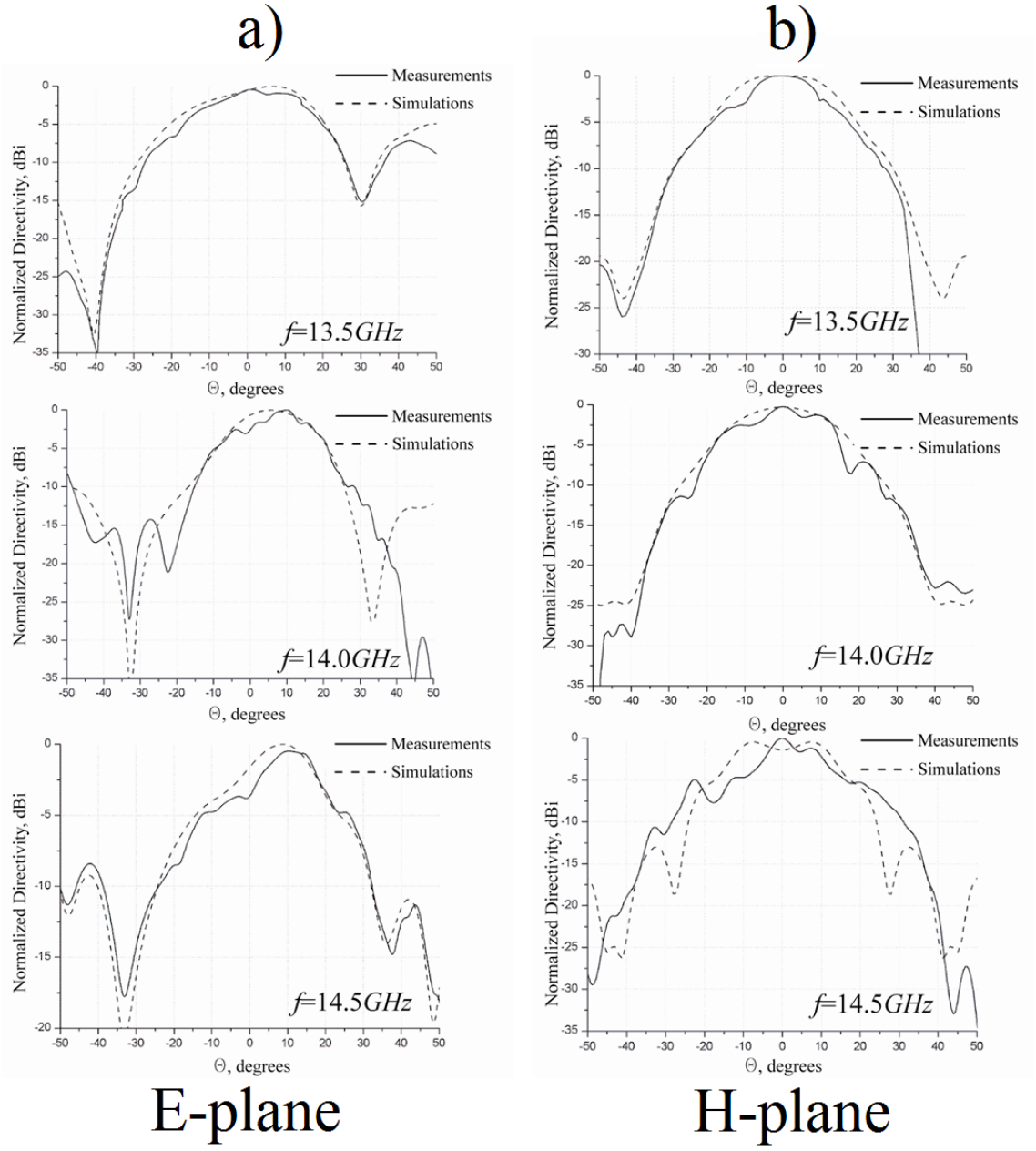

Figure 4.35. Comparison between simulation and measurements [35]

4.4.6 Pyramidal horn antennas

As mentioned above, the most natural sectoral horn antenna which can be created taken as base the woodpile structure is a sectoral H-horn antenna, where the electric field is parallel to the woodpile stacking direction. Thus, the E-plane dimensions of such horn antennas are determined by the thickness of the woodpile bars, since these horns are created within a single woodpile layer. Such a narrow and pre-determined aperture leads to a broad beam in the E-Plane, which is non-symmetrical due to the absence of mirror symmetry in the stacking direction of the woodpile structure.

Reducing the E-plane beamwidth would require creating a pyramidal horn antenna. The difficulty of creating a pyramidal horn based on a defect-containing woodpile structure lies in the complexity of the embedding medium itself. As shown in [36] simple solutions based on cutting several woodpile layers, lead to resonant structures. A solution to his problem can be obtained if the woodpile layers are tilted as shown in Fig. 4.36.

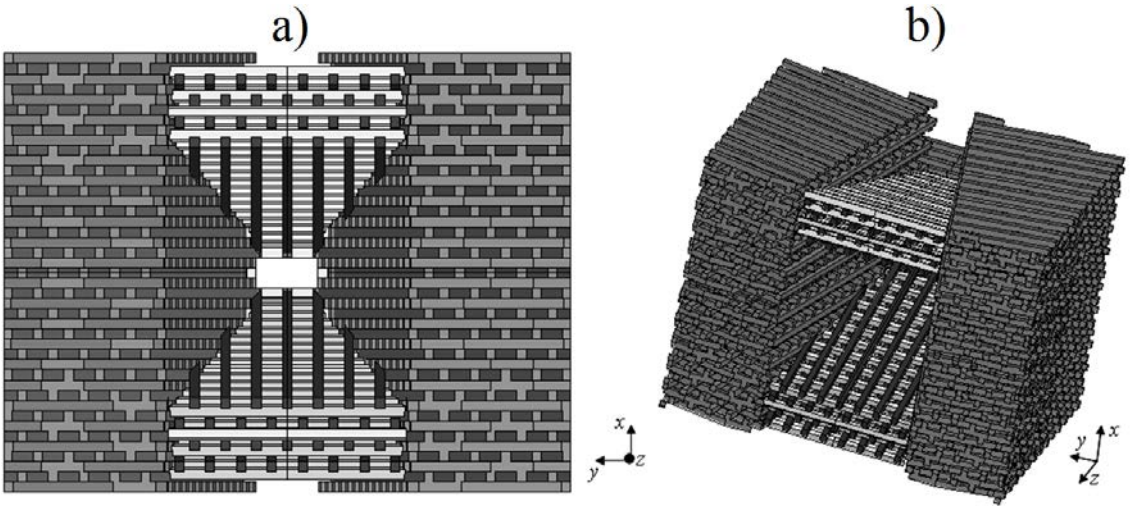

Figure 4.36. Woodpile based symmetrical EH-horn antenna (a – front view, b – 3D view) [36]

This EBG pyramidal horn allows simultaneously controlling the E and H planes of the radiation patterns. An example of the pattern that can be obtained is presented in Fig. 4.37. Its main drawback comes from the manufacturing difficulties, since the layer-by-layer manufacturing approach followed for the woodpile is not valid anymore.

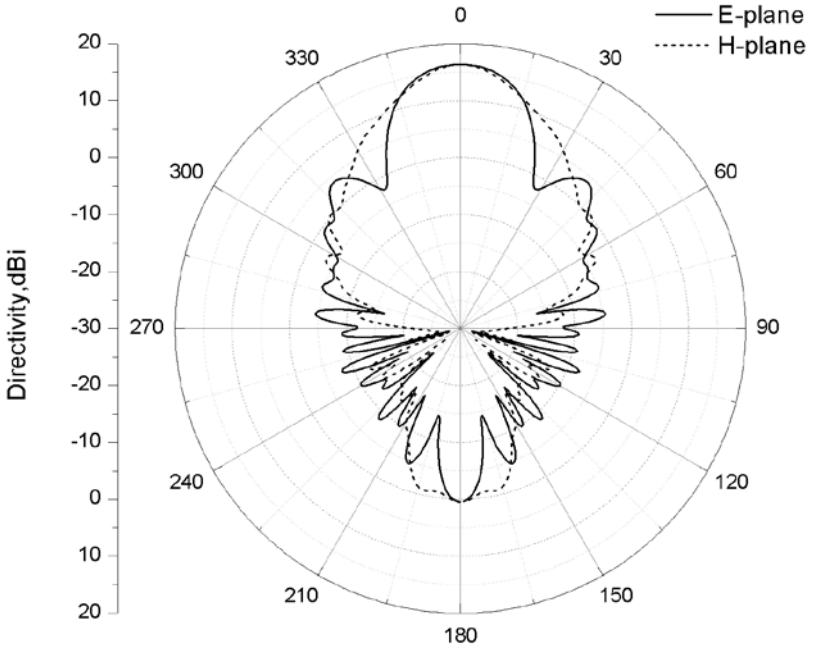

Figure 4.37. Radiation pattern of the EBG pyramidal horn in Fig. 4.36 [36]

References

[1] A.D. Olver, P.J.B. Clarricoats, A.A. Kishk and L. Shafai, "Microwave Horns and Feeds", *IEE Electromagnetic waves series 39*, The Institution of Electrical Engineers, 1994.

[2] P.D. Potter, "A new horn antenna with suppressed sidelobes and equal beamwidths", *Microwave Journal*, 1963, 6, pp. 71-78.

[3] S. Ramo, J.R. Whinnery, T. van Duzer, "Fields and Waves in Communication Electronics", *John Wiley & Sons, Inc.*1994.

[4] Potter, P. D., "A New Horn Antenna with Suppressed Sidelobes and Equal Beamwidths", *Microwave Journal*, vol. VI, June 1963, pp. 71-78.

[5] Clarricoats, P.J.B. and Olver, A.D., "Corrugated Horns for Microwave Antennas", *IEE Electromagnetics Waves Series 18*, Chap. 5, 6 and 7, Peter Peregrinus, 1984.

[6] G.L. James, "Analysis and design of TE_{11} to HE_{11} corrugated cylindrical waveguide mode converters", *IEEE Transactions on Microwave Theory and Techniques*, Vol. MTT-29, pp. 1059-1066, 1981.

[7] B. Maca, Thomas, G.L. James and K.J. Greene, "Design of high-performance wideband corrugated horns for Cassegrain antennas", *IEEE Transactions on Antennas and Propagation*, Vol. AP-34, pp. 750-757, 1986.

[8] Mician μWave Wizard Software, http://www.mician.com

[9] Ticra's CHAMP Software, http://www.ticra.com/products/software/champ

[10] C. Granet and G. L. James, "Design of corrugated horns: a primer," IEEE Antennas and Propagation Magazine. Vol. 47, Issue 2, pp. 76-84, 2005.

[11] R. Gonzalo, J. Teniente and C. del Río, "Improved Radiation Pattern Performance of Horn Antennas with Gaussian Profiled Shapes", IEEE Transactions on Antennas and Propagation, Vol. 50, No. 11, pp. 1505-1513, 2002.

[12] J. Teniente, R. Gonzalo and C. del-Río, "Choked Gaussian Antenna: Extremely Low Sidelobe Compact Antenna Design", IEEE Antennas and Wireless Propagation Letters, Vol. 1, pp. 200-202, 2002.

[13] J. Teniente, A. Martínez, B. Larumbe, A. Ibañez y R. Gonzalo, “Design Guidelines of Horn Antennas that combine Horizontal and Vertical Corrugations for Satellite Communications”, IEEE Transactions on Antennas and Propagation, Vol. 63, No. 4, pp. 1314-1323, 2015.
[14] C. Granet, G. L. James, R. Bolton and G. Moorey, “A smooth-walled spline-profile horn as an alternative to the corrugated horn for wide band millimeter-wave applications”, IEEE Transactions on Antennas and Propagation, Vol. 52, No. 3, pp. 848-854, 2004.
[15] P. D. Potter, “A new horn antenna with suppressed sidelobes and equal beamwidths”, Microwave Journal, Vol. 6, pp. 71–78. 1963.
[16] J., Leech, B. K. Tan and G. Yassin. “Smooth walled feed horns for mm and submm radio astronomy”, 6th UK, Europe, China Millimeter Waves and THz Technology Workshop (UCMMT). 2013.
[17] R.H. Turrin, “Dual Mode Small-Aperture Antennas”, IEEE Transactions on Antennas and Propagation, Vol. 15, No. 2, pp. 307-308, 1967.
[18] J. Leech, B. K. Tan, G. Yassin, P. Kittara, S. Wangsuya, J. Treuttel, M. Henry, M. L. Oldfield and P. G. Huggard, ”Multiple flare-angle horn feeds for sub-mm astronomy and cosmic microwave background experiments”, Astronomy and Astrophysics, Vol. 532, 2011.
[19] J. Teniente, D. Valcázar, B. Larumbe, A. Martínez, A. Ibañez and R. Gonzalo, “Feed Horn Antennas for Data Downlink and Uplink Spaceborne Communications”, 10th European Conference on Antennas and Propagation, EuCAP 2016.
[20] L. Zeng, C. L. Bennett, D. T. Chuss and E. J. Wollack “A Low Cross-Polarization Smooth-Walled Horn with Improved Bandwith”, IEEE Transactions on Antennas and Propagation, Vol. 58, No. 4, 2010.
[21] E. Lier E and P. S. Kildal, “Soft and hard horn antennas”, IEEE Transactions on Antennas and Propagation. Vol. 36, No. 8, pp. 1152–1157, 1988.
[22] E. Lier, “Review of soft and hard horn antennas, including metamaterial-based hybrid-mode horns”, IEEE Antennas and Propagation Magazine, Vol. 52, No. 2, pp. 31–39, 2010.
[23] C. P. Scarborough, Q. Wu, D. H. Werner, E. Lier, R. K. Shaw and B. G. Martin, “Demonstration of an Octave-Bandwidth Negligible-Loss Metamaterial Horn Antenna for Satellite Applications”, IEEE Transactions on Antennas and Propagation, Vol. 61, No. 3, pp. 1081-1088, 2013.
[24] Q. Wu, C. P. Scarborough, B. G. Martin, R. K. Shaw, D. H. Werner, E. Lier and X. Wang, “A Ku-Band Dual Polarization Hybrid-Mode Horn Antenna Enabled by Printed-Circuit-Board Metasurfaces”, IEEE Transactions on Antennas and Propagation. Vol. 61, No. 3, pp. 1089-1098, 2013.
[25] Q. Wu, C. P. Scarborough, D. H. Werner, E. Lier and R. K. Shaw, “Inhomogeneous Metasurfaces With Engineered Dispersion for Broadband Hybrid-Mode Horn Antennas”, IEEE Transactions on Antennas and Propagation. Vol. 61, No. 10, pp. 4947-4956, 2013.
[26] J. D. Joannopoulos, R. D. Meade and J. N. Winn, “Photonic crystals”, Princeton University Press, 1995.
[27] P. de Maagt, R. Gonzalo, J. C. Vardaxoglou and J. M. Baracco, “Photonic bandgap antennas and components for microwave and (sub)millimetre wave applications”, IEEE Transactions on Antennas and Propagation. Vol. 51, No. 10, pp. 2667–2677, 2003.
[28] A. R. Weily, K. P. Esselle and B. C. Sanders, “Photonic crystal horn and array antennas”, Phys. Rev. E. 68, 016609-1-016609-6, 2003.

[29] K. M. Ho, C. T. Chan, C. M. Soukoulis, R. Biswas and M. Sigalas, “Photonic band gaps in three dimensions: New layer-by-layer periodic structures”, Solid State Communicastions, Vol. 89, No. 6, pp. 413-416, 1994.
[30] H. S. Sözüer and J. Dowling, “Photonic Band Calculations for Woodpile Structures”, Journal of Mod. Opt., Vol. 41, No. 2, pp. 231-239, 1994.
[31] R. Gonzalo, B. Martínez, C. M. Mann, H. Pellemans, P. Haring-Bolivar and P. de Maagt, “A low-cost fabrication technique for symmetrical and asymmetrical layer-by-layer photonic crystals at submillimeter-wave frequencies”, IEEE Transactions on Microwave Theory and Techniques, Vol. 50, No. 10, pp. 2384-2392, 2002.
[32] B. Martínez, I. Ederra, R. Gonzalo, B. Alderman, L. Azcona, P. G. Huggard, B. de Hon, A. Hussain, S. R. Andrews, L. Marchand, P. de Maagt, “Manufacturing tolerance analysis, fabrication, and characterization of 3-D submillimeter-wave electromagnetic-bandgap crystals”, IEEE Transactions on Microwave Theory and Techniques, Vol. 55, No.4, pp. 672–681, 2007.
[33] A. R. Weily, K. P. Esselle, B. C. Sanders, “Layer-by-layer photonic crystal horn antenna”, Phys. Rev. E. 70, 037602-4, 2004.
[34] A. R. Weily, K. P. Esselle, T. S. Bird, B. C. Sanders, “Linear Array of Woodpile EBG Sectoral Horn Antennas”, IEEE Transactions on Antennas and Propagation. Vol. 54, No. 8, pp. 2263-2274, 2006.
[35] I. Khromova, I. Ederra, J. Teniente, R. Gonzalo, K.P. Esselle, “Evanescently-Fed Electromagnetic Band Gap Horn Antennas and Arrays”, IEEE Transactions on Antennas and Propagation, Vol. 60, No 6, pp. 2635-2644, 2012.
[36] I. Khromova, I. Ederra, R. Gonzalo, B. P. de Hon, “Symmetrical Pyramidal Horn Antennas Based on EBG Structures”, PIER B 29, 1-22, 2011.